

# Design, evaluation and future projections of the NARClIM2.0 CORDEX-CMIP6 Australasia regional climate ensemble

Giovanni Di Virgilio<sup>1,2</sup>, Jason P. Evans<sup>2,3</sup>, Fei Ji<sup>1,3</sup>, Eugene Tam<sup>1</sup>, Jatin Kala<sup>4</sup>, Julia Andrys<sup>4</sup>, Christopher Thomas<sup>2</sup>, Dipayan Choudhury<sup>1</sup>, Carlos Rocha<sup>1</sup>, Stephen White<sup>1</sup>, Yue Li<sup>1</sup>, Moutassem El Rafei<sup>1</sup>, Rishav Goyal<sup>1</sup>, Matthew L. Riley<sup>1</sup> and Jyothi Lingala<sup>4</sup>

<sup>1</sup>Climate & Atmospheric Science, NSW Department of Climate Change, Energy, the Environment and Water, Sydney, Australia

<sup>2</sup>Climate Change Research Centre, University of New South Wales, Sydney, Australia

<sup>3</sup>Australian Research Council Centre of Excellence for Climate Extremes, University of New South Wales, Sydney, Australia

<sup>4</sup>Environmental and Conservation Sciences, and Centre for Climate Impacted Terrestrial Ecosystems, Harry Butler Institute, Murdoch University, Murdoch, WA 6150, Australia

Correspondence to: Giovanni Di Virgilio ([giovanni.divirgilio@environment.nsw.gov.au](mailto:giovanni.divirgilio@environment.nsw.gov.au); [giovanni@unsw.edu.au](mailto:giovanni@unsw.edu.au))

1 **Abstract.** NARClIM2.0 comprises two Weather Research and Forecasting (WRF) regional climate  
2 models (RCMs) downscaling five CMIP6 global climate models contributing to the Coordinated  
3 Regional Downscaling Experiment over Australasia at 20 km resolution, and south-east Australia at 4  
4 km convection-permitting resolution. We first describe NARClIM2.0's design, including selecting  
5 two, definitive RCMs via testing seventy-eight RCMs using different parameterisations for planetary  
6 boundary layer, microphysics, cumulus, radiation, and land surface model (LSM). We then assess  
7 NARClIM2.0's skill in simulating the historical climate versus CMIP3-forced NARClIM1.0 and  
8 CMIP5-forced NARClIM1.5 RCMs and compare differences in future climate projections. RCMs  
9 using the new Noah-MP LSM in WRF with default settings confer substantial improvements in  
10 simulating temperature variables versus RCMs using Noah-Unified. Noah-MP confers smaller  
11 improvements in simulating precipitation, except for large improvements over Australia's southeast  
12 coast. Activating Noah-MP's dynamic vegetation cover and/or runoff options primarily improve  
13 simulation of minimum temperature. NARClIM2.0 confers large reductions in maximum temperature  
14 bias versus NARClIM1.0 and 1.5 (1.x), with small absolute biases of ~0.5K over many regions versus  
15 over ~2K for NARClIM1.x. NARClIM2.0 reduces wet biases versus NARClIM1.x by as much as  
16 50%, but retains dry biases over Australia's north. NARClIM2.0 is biased warmer for minimum  
17 temperature versus NARClIM1.5 which is partly inherited from stronger warm biases in CMIP6

18 versus CMIP5 GCMs. Under shared socioeconomic pathway (SSP)3-7.0, NARcliM2.0 projects ~3K  
19 warming by 2060-79 over inland regions versus ~2.5K over coastal regions. NARcliM2.0-SSP3-7.0  
20 projects dry futures over most of Australia, except for wet futures over Australia's north and parts of  
21 western Australia which are largest in summer. NARcliM2.0-SSP1-2.6 projects dry changes over  
22 Australia with only few exceptions. NARcliM2.0 is a valuable resource for assessing climate change  
23 impacts on societies and natural systems and informing resilience planning by reducing model biases  
24 versus earlier NARcliM generations and providing more up-to-date future climate projections  
25 utilising CMIP6.

**Keywords:**

26 Climate change; climate impact adaptation; dynamical downscaling; CORDEX-CMIP6; model  
27 design; model evaluation

## 28 **1. Introduction**

29 Climate projections are foundational to informing climate change mitigation and adaptation planning  
30 at various spatial scales (IPCC, 2021). Regional climate models (RCMs) dynamically downscale  
31 global climate models (GCMs) at ~100-200 km resolution to simulate higher resolution climate  
32 projections that better resolve local-scale influences on regional climate, such as mountain ranges,  
33 land-use variation, land-sea contrasts, and convective processes (Torma et al., 2015; Giorgi, 2019). As  
34 such, whilst GCMs are the best tools for investigating climate at global scales, RCMs provide  
35 improved guidance for climate policy at regional scale, which is the scale at which climate change  
36 impacts are experienced (Hsiang et al., 2017).

37 The NARcliM programme (New South Wales and Australian Regional Climate Modelling) is  
38 now in its third generation. Like its predecessors, NARcliM version 2.0 ('NARcliM2.0'), aims to  
39 produce robust, detailed regional climate projections at spatial scales relevant for use in local-scale  
40 climate change analysis. A key feature of all NARcliM generations is to simulate the climate over the  
41 Coordinated Regional Downscaling Experiment (CORDEX)-Australasia domain, and a higher  
42 resolution inner domain over southeast Australia via one-way nesting (Figure 1). With one-way  
43 nesting the inner domain obtains its initial and lateral boundary conditions from the simulation over  
44 CORDEX-Australasia. NARcliM1.0 simulated the climate of Australasia for three periods (1990-  
45 2009, 2020-2039, 2060-2079) at 50 km resolution and southeast Australia at 10 km using three  
46 configurations of the weather research and forecasting (WRF) RCM (Skamarock et al., 2008) to  
47 downscale GCMs from Coupled Model Intercomparison Project phase three (CMIP3) under the SRES  
48 A2 greenhouse gas (GHG) scenario (Evans et al., 2014). NARcliM1.5 used CMIP5 GCMs under  
49 representative concentration pathways (RCP) 4.5 and 8.5 to simulate continuously for 1950-2100 on  
50 the same grids as NARcliM1.0 using two of its RCMs (Nishant et al., 2021).

51 NARcliM2.0 aims to improve performance in simulating the Australian climate relative to  
52 previous NARcliM generations with the goal of better informing community resilience to climate  
53 change (New South Wales Government, 2022, 2023). All NARcliM projects include a bottom-up  
54 design ethos involving multi-sectoral end-user engagement in specifying model requirements to  
55 ensure model performance and outputs meet end-user needs. Key requirements from the NARcliM2.0  
56 user-consultation include providing increased detail in climate simulations via higher resolution and  
57 improving the simulation of precipitation and temperature as these are fundamental inputs to climate  
58 impact studies. Whilst NARcliM1.0 and 1.5 (1.x) confer the expected level of performance in  
59 simulating the Australian climate (Di Virgilio et al., 2019; Evans et al., 2020b), recent technological  
60 and scientific advancements mean that aspects of their performance might now be improved.  
61 NARcliM1.x RCMs show widespread cold biases in maximum temperature exceeding -5K for some  
62 RCMs. Conversely, minimum temperature is simulated more accurately with biases in the range of

63  $\pm 1.5K$ . NARClIM1.x RCMs overestimate precipitation, particularly over Australia's socio-  
64 economically important eastern seaboard (Di Virgilio et al., 2019).

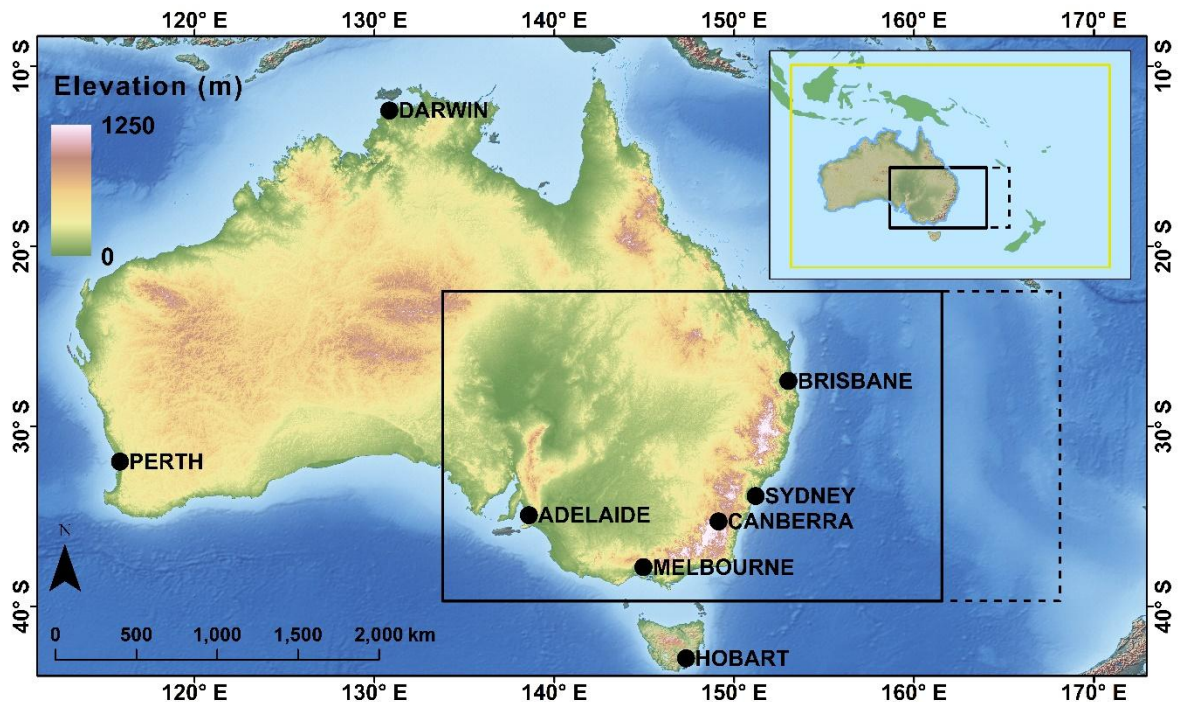
65 As they are expensive to run from both computational and data storage perspectives, dynamical  
66 downscaling projects like NARClIM2.0 use a subset of available GCMs as driving data, necessitating  
67 careful model selection. Similarly, a large combination of different physical parametrisations  
68 available for the WRF RCM enables many structurally different RCMs to be potentially used to  
69 downscale GCMs. A key component of NARClIM2.0's design is testing the viability of alternative  
70 RCM parameterisations via a three-phase approach, with each phase building on the preceding phase  
71 to identify the RCM parameterisations that perform well during testing to meet NARClIM2.0's aim of  
72 improving the simulation of Australia's climate. GCM and RCM statistical independence are also  
73 sought to avoid creating a biased sample of climate change. Hence, the aims of this paper are to:

74 1) describe how and why NARClIM2.0 differs from its predecessors in terms of its design and  
75 production processes, explaining the model test and evaluation approaches underlying its design  
76 decisions. A key focus is on the design and testing of seventy-eight structurally different WRF RCMs  
77 and their evaluation to identify a subset of RCMs for use in NARClIM2.0;

78 2) characterise the performance improvements of CMIP6-NARClIM2.0 RCMs in simulating the  
79 Australian climate relative to previous NARClIM generations by evaluating their skill in simulating  
80 mean maximum and minimum temperature and precipitation versus observations;

81 3) summarise the climate projections produced by CMIP6-NARClIM2.0 and how these differ  
82 from previous CMIP3-5-NARClIM generations.

83 The following section summarises the basic design features of each NARClIM generation;  
84 Section 3. describes evaluation methods and metrics; Section 4. describes NARClIM2.0's design  
85 process with a focus on its RCM physics testing, as well as a brief overview of its production process;  
86 Section 5. summarises the RCM physics test results; Section 6. evaluates the performance of all  
87 NARClIM models in simulating the recent Australian climate; Section 7. provides an overview of  
88 their future projections; and Section 8. discusses key results and summarises this paper.



89

90 **Figure 1.** Model domains for NARClIM regional climate simulations. The southeast inner domain for  
 91 NARClIM2.0 is delineated with a solid black rectangle; the corresponding inner domain for NARClIM1.0 and  
 92 1.5 is delineated with a dashed black line. The elevated terrain of the Australian Alps which form part of the  
 93 Great Dividing Range is in eastern Australia. Inset shows the CORDEX-Australasia outer domain.

## 94 **2. Three generations of NARClIM: model overviews**

95 The design of NARClIM1.0 is described in Evans et al. (2014); NARClIM1.5 used the same design  
 96 approach but used CMIP5 rather than CMIP3 GCMs. All generations of NARClIM use different  
 97 versions of the WRF model to perform dynamical downscaling of GCMs since the WRF model goes  
 98 through regular updates. The southeast Australian inner domain captures five of Australia's eight  
 99 capital cities (Figure 1) and over 75% of the Australian population (Australian Bureau Statistics,  
 100 2024). Additionally, the inner domain captures coastal regions that are characterised by topographic  
 101 complexity and land-use class variation. Regions east of the Great Dividing Range mountains in  
 102 southeast Australia (Figure 1) show different responses to oceanic climate modes compared to inland  
 103 semi-arid regions (Murphy and Timbal, 2008) and are impacted by events such as rapidly developing  
 104 storms, including east coast lows (Pepler and Dowdy, 2021). Such atmospheric processes are not  
 105 adequately resolved by GCMs due to coarse resolutions (Di Virgilio et al., 2022; Grose et al., 2020).

106 NARClIM2.0 encompasses several design advancements over its predecessors (Table 1).  
 107 NARClIM2.0 RCMs have a 20 km resolution CORDEX-Australasia domain (versus 50 km) and 4 km  
 108 (versus 10 km) domain over southeast Australia and use 45 (versus 30) vertical levels. The aim of  
 109 increasing the resolution of this inner domain from 10 km to 4 km is to render these simulations

110 convection-permitting (Kendon et al., 2021; Lucas-Picher et al., 2021). Hence, whilst the 20 km-  
111 resolution outer domain uses cumulus parametrisation, simulations over the 4 km domain do not use  
112 cumulus parametrisation. NARClIM2.0 also includes a new collaboration with the Western Australian  
113 government, with separate 4 km simulations being performed over south-west and north-west Western  
114 Australia (not shown in Figure 1) as part of the Western Australian climate science initiative (DWER,  
115 2023). Boundary conditions derived from the 20 km NARClIM2.0 CORDEX Australasia domain are  
116 used to drive these simulations. Additional major differences in model setup for NARClIM2.0  
117 include:

- 118     ▪ NARClIM1.0 RCMs use different parameterisations for planetary boundary layer (PBL)  
119     physics, surface physics, cumulus physics, land surface model (LSM), and radiation (Evans et  
120     al., 2014). These RCM parameterisations were also used for NARClIM1.5. Owing to the pro-  
121     ject aims stated above, RCM parameterisations for NARClIM2.0 differ to those of NAR-  
122     ClIM1.x (see Sect. 4).
- 123     ▪ NARClIM2.0 increases the number of driving GCMs to 5 and simulates for a wider range of  
124     plausible future climates via three shared socioeconomic pathways (SSP). SSP1-2.6 is se-  
125     lected as a low GHG scenario envisaging a future climate with CO<sub>2</sub> emissions cut to net zero  
126     by around 2075 and warming held to below 2°C by 2100; SSP2-4.5 estimates projected  
127     warming under a ‘middle of the road’ scenario where temperatures increase to ~2.7°C by  
128     2100; and SSP3-7.0 is a high GHG scenario which assumes warming of ~4°C by 2100 (IPCC,  
129     2021).
- 130     ▪ Urban physics is activated in NARClIM2.0 (WRF setting: sf\_urban\_physics=1) to represent  
131     surface energy balance in urban areas via a single layer urban canopy model (Kusaka and  
132     Kimura, 2004).
- 133     ▪ Input of different aerosol species is activated for the RCM radiation scheme using the Tegen  
134     et al. (1997) climatology available in WRF (aer\_opt=1). This aerosol forcing is the same for  
135     all GCMs, and not model-specific.
- 136     ▪ The eastern boundary of the NARClIM2.0 inner domain is located further westward relative  
137     to that of NARClIM1.x (Figure 1).

138 **Table 1.** High-level design features of three generations of NARClIM regional climate models

|  | <b>Model Generation</b>            |                                      |                                    |
|--|------------------------------------|--------------------------------------|------------------------------------|
|  | NARClIM1.0                         | NARClIM1.5                           | NARClIM2.0                         |
| <b>Release date</b>  | 2014                               | 2020                                 | 2023-2024                          |
| <b>Years simulated</b>   | 1990-2009, 2020-2039,<br>2060-2079 | 1950-2100                            | 1950-2100                          |
| <b>Grid resolutions:<br/>CORDEX-Australasia;<br/>NARClIM inner domains</b> | 50 km; 10 km                       | 50 km; 10 km                         | 20 km; 4 km                        |
| <b>Vertical levels</b>   | 30                                 | 30                                   | 45                                 |
| <b>Global Climate Models</b>   | 4 CMIP3 GCMs                       | 3 CMIP5 GCMs                         | 5 CMIP6 GCMs                       |
| <b>Regional Climate Models</b>   | 3 RCM configurations<br>(WRF3.3)   | 2 RCM configurations<br>(WRF3.6.0.5) | 2 RCM configurations<br>(WRF4.1.2) |
| <b>Future emission scenarios</b>   | SRES A2                            | RCP4.5, RCP8.5                       | SSP1-2.6, SSP2-4.5,<br>SSP3-7.0    |
| <b>Reanalysis-driven<br/>(CORDEX Evaluation)</b>                           | NCEP: 1950-2009                    | ERA-Interim: 1979-2013               | ERA5: 1979-2020                    |
| <b>Computational resources<br/>(core hours)</b>                            | 30M                                | 30M                                  | 1060M                              |

### 139 **3. Evaluation methods**

140 This section largely focuses on the methods and metrics used for the NARClIM2.0 RCM physics test-  
141 ing and comparisons of model biases and future climate projections against previous generations of  
142 NARClIM. Details on methods and results for the CMIP6 GCM evaluation used to select driving  
143 GCMs and the ERA5-NARClIM2.0 RCM evaluation used to select two, definitive RCMs for the  
144 GCM-driven simulations are available in Di Virgilio et al. (2022) and Di Virgilio et al. (2024), respec-  
145 tively, with overviews of these components of NARClIM2.0 design provided in Sections 4.2 and 4.4  
146 below.

### 147 **3.1 Observations**

148 Australian Gridded Climate Data (AGCD version 1.0; Evans et al., 2020a) are the observational data  
149 used to evaluate the NARClIM2.0 RCM physics test RCMs. These daily gridded data for maximum  
150 and minimum temperature and precipitation are obtained from an interpolation of station observations  
151 across Australia. AGCD data are on a regular WGS84 grid with a grid-averaged resolution of 0.05°.  
152 For the NARClIM2.0 RCM physics tests, the AGCD data were re-gridded to correspond with the  
153 RCM data from the inner domain on their native grids using a conservative area-weighted re-gridding  
154 scheme. All data (RCM and AGCD) were restricted to a common extent contained within the inner  
155 domain over southeast Australia, and a land mask was applied so that statistics were computed using  
156 only land pixels. Treatment of AGCD for the CMIP6 GCM evaluation and the ERA5-NARClIM2.0  
157 RCM evaluation is described in Di Virgilio et al. (2022) and Di Virgilio et al. (2024), respectively.

### 158 **3.2 Methods and metrics: phase I-III NARClIM2.0 physics tests**

159 Test RCM performances in reproducing observations for daily maximum and minimum temperature  
160 and daily precipitation were assessed by calculating the model bias, i.e., model outputs minus AGCD,  
161 and the RMSE of modelled versus observed fields. Model biases and RMSEs were calculated at an-  
162 nual and seasonal timescales. The model representations of the hottest and the wettest day on an  
163 annual time scale over the study region were also compared with AGCD. Probability density functions  
164 (PDFs) were calculated for each variable using daily data. The Perkins skill score (PSS) (Perkins et  
165 al., 2007) was calculated to assess the overall degree of overlap between modelled and observed dis-  
166 tributions, with  $PSS = 1$  indicating that distributions overlap perfectly.

167 There are several methods to evaluate the overall performance of RCMs. In this study, we  
168 ranked the RCMs individually based on their bias, RMSE, and PSS for maximum temperature, mini-  
169 mum temperature, and precipitation. Each variable was ranked separately for each metric. The ranks  
170 were then summed to determine the overall ranking for each RCM.

### 171 **3.3 Independence assessments**

172 We used the method of Bishop and Abramowitz (2013) as one of two methods of assessing the inde-  
173 pendence of physics test RCMs and the target CMIP6 GCMs under evaluation for use in NAR-  
174 ClIM2.0. This approach uses the covariance in model errors as the basis to define model dependence;  
175 specifically, independence coefficients are derived from the error covariance matrix of the RCMs or  
176 GCMs. Model independence is quantified using the correlation of model errors. For the physics test  
177 RCMs, errors are computed by comparing the climatology of maximum and minimum temperature  
178 and precipitation over the south-east Australia inner domain for 2016 with corresponding AGCD ob-  
179 servations. The same calculation is performed for the CMIP6 GCMs, except for the Australian



180 continent. Daily timeseries of precipitation, maximum and minimum temperature are calculated indi-  
181 vidualy for each RCM and for AGCD. The simulated and observed daily timeseries of each variable  
182 are then normalised by the standard deviation of the corresponding observed variable. These normal-  
183 ised variables are concatenated for each RCM (GCM) and AGCD. An anomaly time series for each  
184 grid cell is then produced. These time series are used to create a model error covariance matrix con-  
185 taining the errors for all RCMs (GCMs). The coefficients of a linear combination of the RCMs  
186 (GCMs) that optimally minimises the mean square error depends on both model performance and  
187 model dependence (Bishop and Abramowitz, 2013). The result of this minimisation problem is writ-  
188 ten in terms of the covariance matrix. The magnitude of coefficients assigned to each RCM (GCM)  
189 reflects a combination of their performance and independence. Highly independent models have dif-  
190 ferent errors when simulating the recent climate. Models with the largest coefficients have the most  
191 independent errors versus observations.

192 The Herger method of subset selection (Herger et al., 2018), as implemented here, uses quad-  
193 ratic integer programming to find the subset of models whose equally-weighted subset mean (EWSM)  
194 minimises a quadratic cost function. This cost function is chosen to measure the performance of the  
195 EWSM in comparison to a given observational product. The two cost functions used here are: the  
196 mean squared error (MSE) between the EWSM and the observational product (Herger et al. 2018, Eq.  
197 1); and another which measures a combination of the MSE of the EWSM, the average MSE of each  
198 subset member, and the average pairwise mean squared distance between subset members (Herger et  
199 al. 2018, Eq. 2).

## 200 **3.4 NARcliM2 CMIP6-RCMs: historical evaluation and climate change** 201 **projections**

202 Performances of NARcliM2.0 versus NARcliM1.x RCMs in reproducing the recent Australian cli-  
203 mate are evaluated by calculating the model biases (model outputs minus AGCD observations) for  
204 mean maximum and minimum temperature and precipitation for 1990-2009. To enable comparison of  
205 future projections between NARcliM1.0, NARcliM1.5 and NARcliM2.0 (where NARcliM1.0 mod-  
206 elled for 1990-2009, 2020-2039, and 2060-2079), all NARcliM ensemble projected changes are  
207 shown as far future (2060–2079) minus present day (1990–2009).

## 208 **3.5 Statistical significance**

209 When quantifying RCMs' future climate change projections (compared to the historical period) and  
210 biases in maximum and minimum temperature, the statistical significance is calculated for each grid  
211 cell using t-tests assuming equal variance. The Mann–Whitney U test is used for precipitation given  
212 its non-normality. Significance thresholds were adjusted to account for multiple testing using  
213 Walker's test (Eq.2 in Wilks, 2016). For individual RCMs, grid cells showing statistically significant

214 changes are stippled, otherwise they are shown in colour where change is statistically insignificant.  
215 Results on the statistical significance of each ensemble mean are separated into three categories fol-  
216 lowing Tebaldi et al. (2011): 1) statistically insignificant areas are shown in colour, denoting that less  
217 than 50% of RCMs are significantly biased/different; 2) in areas of significant agreement (stippled), at  
218 least 50% of RCMs are significantly biased/different and at least 70% of significant models in the  
219 CMIP6-NARClIM2.0 RCM ensemble agree on the sign of the bias/difference. In such areas, many  
220 ensemble members have the same bias sign which is an undesirable outcome; and 3) areas of signifi-  
221 cant disagreement, where at least 50% of RCMs are significantly biased/different and fewer than 70%  
222 of significant models agree on the bias sign, are shown with diagonal hatching for the CMIP6-NAR-  
223 ClIM2.0 historical evaluation and climate change signals.

## 224 4. NARClIM2.0 design and production process overview

225 The NARClIM2.0 design and production processes are summarised below in reference to Figure 2.  
226 The design process is an adaptation of that introduced in Evans et al. (2014). Two companion  
227 manuscripts describe elements shown in Figure 2, which are therefore only summarised briefly in this  
228 manuscript: Di Virgilio et al. (2022) describes the CMIP6 GCM selection process summarised in Box  
229 2, and Di Virgilio et al. (2024) describes the ERA5-RCM evaluation undertaken in Boxes 5 and 6.

### 230 I. Design Phase:

- 231 i) **Box 1:** model design requirements are identified via consultation between NARClIM2.0  
232 modelling groups and multi-sectoral end-users, as well as adherence to CORDEX-CMIP6  
233 design requirements (WCRP, 2020).
- 234 ii) **Box 2:** NARClIM1.x selected driving CMIP3-5 GCMs (respectively) via literature review  
235 of existing GCM evaluations. During NARClIM2.0 design, there were no pre-existing  
236 comprehensive evaluations of individual CMIP6 GCMs for the Australian region, includ-  
237 ing assessments of climate change signals and GCM statistical independence. Hence, an  
238 evaluation and selection of CMIP6 GCMs was conducted (see Di Virgilio et al. 2022).  
239 This evaluation selected five GCMs to force two NARClIM2.0 RCMs (see Sect 4.2 and  
240 4.4). The relative contribution to uncertainty/variation in climate projections can be larger  
241 for GCMs than for RCMs (e.g. Lee et al., 2023).
- 242 iii) **Boxes 3-4:** a new WRF RCM multi-physics test ensemble is created for NARClIM2.0:  
243 RCM physics testing is conducted via a three-phase approach, with each phase building  
244 on the findings of the preceding phase to identify the RCM parameterisations that perform  
245 well during testing with the aim of improving the simulation of the Australian climate. In  
246 this way, RCMs are parameterised with different physics settings via each test phase, sys-  
247 tematically removing poor performing options while facilitating the fine tuning and im-  
248 provement of the parameterisations that perform well during testing to build a total

249 ensemble size of seventy-eight structurally different test RCMs. The performance of the  
250 different test RCM configurations is evaluated, ultimately leading to the selection of a  
251 subset of seven RCMs for subsequent downscaling of ERA5 reanalysis as part of the  
252 CORDEX evaluation experiment.

253 iv) **Boxes 5-6:** These seven RCMs are used to downscale ERA5 reanalysis over the 20 km  
254 and 4 km domains for 1979-2020. Evaluating these ERA5-forced simulations informs se-  
255 lection of two definitive, production RCMs for CMIP6-forced downscaling (see Sect. 4.4  
256 and Di Virgilio et al. 2024).

## 257 II. Production Phase:

258 i) **Boxes 7-8:** CMIP6 GCM data are pre-processed to create initial and boundary conditions  
259 to drive simulations for the historical (1950-2014) and SSP experiments (2015-2100). A  
260 code repository used for this GCM preprocessing is available on Zenodo at:

261 <https://doi.org/10.5281/zenodo.11184830> within the WRF/repo\_snapshots subdirectory.

262 Quality assurance/quality control (QA/QC) is performed on these data before initiating  
263 the simulations (e.g. variables are checked to confirm data do not contain significant out-  
264 liers across ensemble members).

265 ii) **Boxes 9-11:** the 151-year CMIP6-forced NARClIM2.0 RCM simulations are run using  
266 National Computational Infrastructure at Canberra, Australia (NCI, <https://nci.org.au/>).  
267 File integrity verification and QA/QC are performed on each year of raw WRF output  
268 throughout the simulation lifecycle and prior to post-processing to CORDEX-compliant  
269 format climate variables. QA/QC tests include calculating the minimum, maximum, mean  
270 and standard deviation for key variables over consecutive periods of six simulation days.  
271 Variables are categorised as either normally distributed or otherwise. Normally distrib-  
272 uted variables (e.g. surface temperature) are deemed potentially erroneous if their min-  
273 ima/maxima are greater than five standard deviations away from the global mean of the  
274 relevant statistic of the rolling six-day period. Non-normally distributed variables (e.g.,  
275 snow depth and precipitation) are checked only for global minima and maxima.

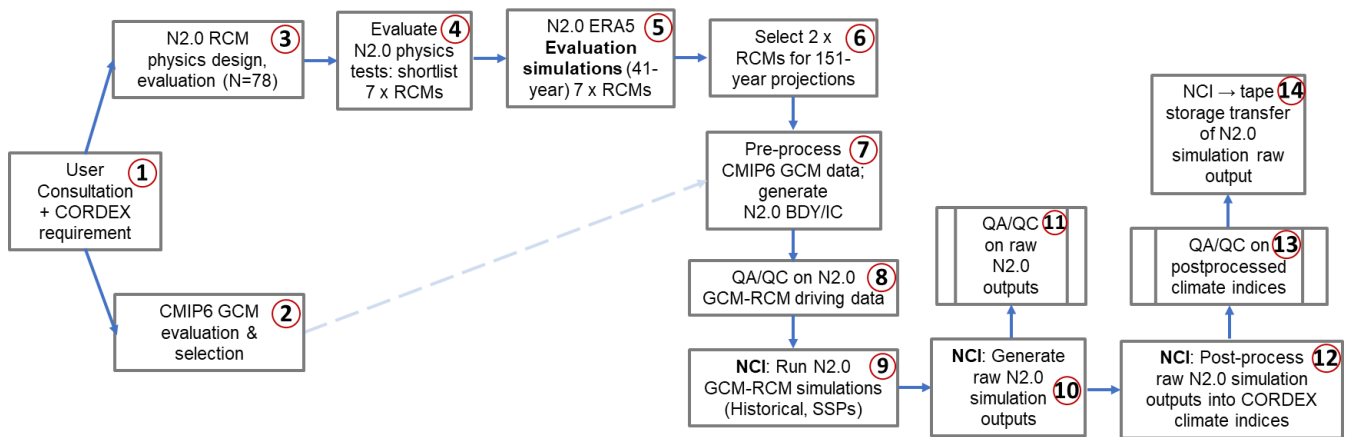
276 iii) **Boxes 12-13:** after each year of simulation raw output is generated, their post-processing  
277 is initiated to produce CORDEX CORE, Tier 1 and Tier 2 variables (WCRP, 2022). A  
278 statistical QA/QC process is automatically applied to each year of post-processed  
279 CORDEX CORE variables as they are generated throughout the simulations. QA/QC  
280 tests include:

- 281     ▪ Check for presence of missing values.
- 282     ▪ Check that all values are within realistic ranges for minima and maxima.
- 283     ▪ Check minima and maxima are not equal at any timestep with exceptions (e.g.,  
284         snow depth which can be zero everywhere in the outer domain).

- 285                   ▪ Check that changes over time are within realistic ranges (i.e., assess temporal gra-
- 286                   dients).
- 287                   ▪ Check that changes between neighbouring data points are within realistic ranges
- 288                   (i.e., assess spatial gradients).
- 289                   ▪ Check the number of grid cells with NaN (non-numerical) values do not exceed
- 290                   the threshold set for the variable.

291 Reasonable ranges for variables are determined using a series of threshold values that are  
 292 based on historical records and/or empirical analysis. QA/QC computer scripts generate  
 293 exceedance files which output every data point that surpasses the threshold values, and  
 294 these exceedance files are then manually reviewed to determine whether an issue is a true  
 295 or false positive, etc.

296 iv) **Box 14:** Once each year of WRF raw files is post-processed, raw files are transferred to a  
 297 tape facility for long-term storage.



298  
 299 **Figure 2.** Simplified overview of NARClM2.0 (N2.0) design and production processes. ERA5 = ECMWF  
 300 Reanalysis v5 data; BDY = boundary conditions; IC = Initial conditions; QA/QC = Quality Assurance / Quality  
 301 Control; NCI = National Computational Infrastructure (high performance computer used to run N2.0  
 302 simulations).

303 These model design and production stages are now described in more detail:

### 304 4.1 Model evaluation and selection

305 Practical constraints such as available compute and data storage resources enforce an upper limit on  
 306 GCM-RCM ensemble size. Thus, NARClM2.0 uses a subset of available CMIP6 GCMs and WRF  
 307 RCM configurations, necessitating careful GCM and RCM selection to create a subset of GCM-  
 308 RCMs that provide robust climate simulations whilst also adequately sampling model uncertainty. In  
 309 selecting a subset of GCMs and RCMs for dynamical downscaling, it is desirable to reject models that

310 perform consistently poorly relative to their peers in simulating the current climate, as this provides  
311 lower confidence in the projected change (Evans et al., 2020b; Di Virgilio et al., 2022; Grose et al.,  
312 2023). Furthermore, the modelled climate space sampled is reduced when selecting a subset of GCMs,  
313 which can create a biased view of the climate, as well as the plausible change in climate. Care must  
314 therefore be taken to ensure that the subset of models used for downscaling are representative of the  
315 full range of possible climates, and that model errors are uncorrelated, i.e., that models are statistically  
316 independent. The steps taken to evaluate and select GCMs and RCMs for NARClIM2.0 are described  
317 next.

## 318 **4.2 CMIP6 GCM evaluation**

319 A three-phase process was used to evaluate individual CMIP6 GCMs (for further details see Di  
320 Virgilio et al. 2022):

### 321 **4.2.1 CMIP6 GCM Performance**

322 We evaluated the performances of individual CMIP6 GCMs in simulating the following aspects of the  
323 observed historical climate of Australia:

- 324     ▪ annual and seasonal climatologies and daily distributions of maximum and minimum temper-  
325     atures and precipitation.
- 326     ▪ climate extremes, such as the 99<sup>th</sup> percentiles of daily maximum temperature and precipita-  
327     tion, and the 1<sup>st</sup> percentile of minimum temperature.
- 328     ▪ teleconnections of oceanic climate modes and Australian regional rainfall.

329 Temperature and precipitation variables are chosen for evaluation because, being well-represented in  
330 high-quality gridded observational data sets for the Australian continent, they provide the most direct  
331 comparison to observations (King et al., 2013). They are also often prioritised for impact studies.  
332 Given variables such as winds (U, V), air temperature (T), water mixing ratio (Q), geopotential height  
333 (Z), sea surface temperature (SST), and sea level pressure (PSL) serve as boundary conditions for  
334 driving RCMs, these could be incorporated into future GCM evaluation studies. However, evaluating  
335 such variables would require use of re-analysis data as surrogate observations.

336         A set of GCMs that performed consistently poorly across the variables and statistics  
337 considered were identified. These models, as well as those with insufficient data to enable dynamical  
338 downscaling using the WRF RCM, were excluded from further evaluation leaving 27 GCMs for  
339 subsequent assessment.

#### 340 **4.2.2 CMIP6 GCM Independence**

341 The retained 27 GCMs were subjected to the Bishop and Abramowitz (2013) and Herger et al. (2018)  
342 independence analyses (see Sect. 3.5). The GCMs were then ranked according to their relative level of  
343 statistical independence.

#### 344 **4.2.3 Sampling CMIP6 GCM Climate Change Spread**

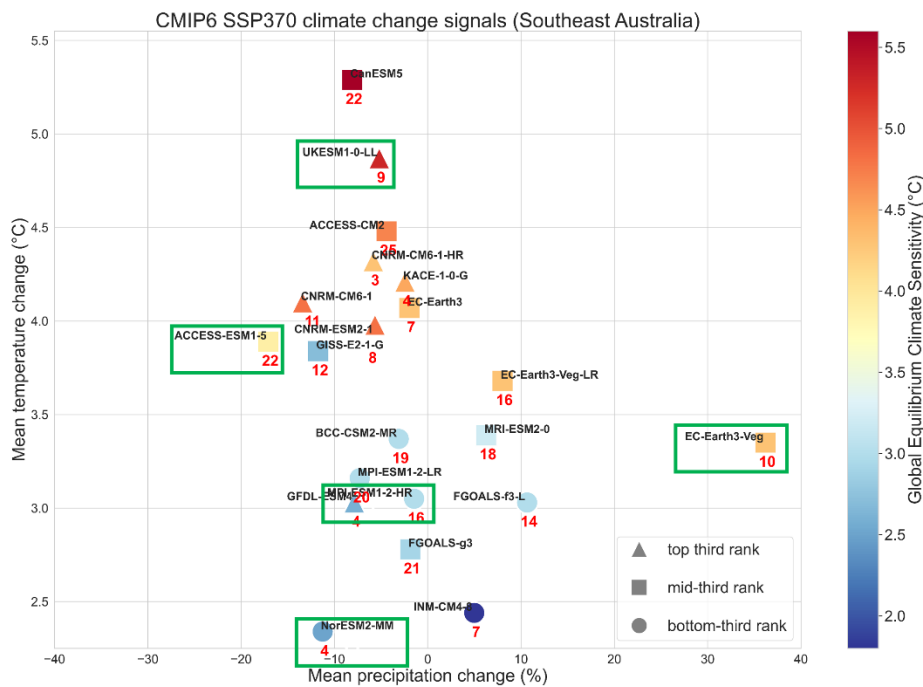
345 For climate change risk assessments, climate projections should reflect as much of the range of  
346 plausible future climate changes as possible (Whetton and Hennessy, 2010). The subset of CMIP6  
347 GCMs selected for NARClIM2.0 spanned a wide range of future changes in annual mean temperature  
348 and precipitation. Climate change signals were calculated for 2080-2099 minus 1995-2014 for the  
349 Australian continent and south-east Australia under SSP3-7.0 (for the latter, see Figure 3). The GCM  
350 independence rankings were placed within this climate change space, with higher independence  
351 rankings viewed as favourable, along with consideration of the following criteria:

- 352 i) A balanced range of GCM Equilibrium Climate Sensitivities (ECS) were sampled. ECS is the  
353 long-term increase in global mean surface air temperature in response to the radiative forcing  
354 caused by a doubling of pre-industrial CO<sub>2</sub> concentrations. ECS is related to global tempera-  
355 ture change, not just changes over Australia, however, it correlates strongly with regional  
356 warming. Around one third of CMIP6 GCMs show ECS values higher than the upper end of  
357 the likely range of 2.5°C to 4°C (IPCC, 2021). An upper range of > ~5°C cannot be ruled out  
358 (Meehl et al., 2020; Bjordal et al., 2020; Sherwood et al., 2020).
- 359 ii) Some CMIP6 GCMs that are favourable in terms of model performance and independence  
360 could not be selected as input to WRF for NARClIM2.0 owing to insufficient data availability  
361 for key variables, where ideally, WRF requires sub-daily data for the variables shown in Sup-  
362 porting Information, Table S1.

363 As a result of the above process, the five CMIP6 GCMs listed in Table 2 are selected to force each of  
364 the two definitive NARClIM2.0 RCMs selected via the RCM physics testing and ERA5 evaluation  
365 processes.

366 **Table 2.** Basic details of the CMIP6 GCMs used to force the two definitive RCMs comprising the  
367 NARClIM2.0 CORDEX-CMIP6 ensemble.

| CMIP6 GCM     | Institution                                | Variant/Run | Atmosphere lat/lon grid (°) |
|---------------|--|-------------|-----------------------------|
| ACCESS-ESM1-5 | CSIRO                                      | r6i1p1f1    | 1.2 × 1.8                   |
| EC-Earth3-Veg | EC-EARTH consortium                        | r1i1p1f1    | 0.7 × 0.7                   |
| MPI-ESM1-2-HR | Max Planck Institute for Meteorology (MPI) | r1i1p1f1    | ~0.9                        |
| NorESM2-MM    | Norwegian Climate Centre                   | r1i1p1f1    | 0.9 × 0.9                   |
| UKESM1-0-LL   | UK Met Office and NERC research centres    | r1i1p1f2    | 1.3 × 1.9                   |



368  
 369 **Figure 3.** CMIP6 GCM climate change signals (2080-2099 versus 1995-2014) over south-east Australia for the  
 370 subset of GCMs retained following the model performance evaluation in Di Virgilio et al. (2022), and that  
 371 simulated at least monthly mean near surface air temperature and precipitation for the SSP-3.70 scenario. Boxed  
 372 GCMs are selected to force NARcliM2.0 RCMs. Marker shapes indicate overall GCM performance; markers  
 373 are coloured according to their global equilibrium climate sensitivity (ECS) values; **Red** numbers represent the  
 374 smallest Herger Method 1 set for that GCM.

### 375 4.3 NARcliM2.0 RCM physics testing

376 The NARcliM2.0 RCM physics testing aims to identify and exclude RCMs that perform consistently  
 377 poorly in simulating the southeast Australian climate and to select RCMs that have high statistical  
 378 independence. The selection of RCMs in NARcliM2.0 involves the creation of a multi-physics  
 379 ensemble where each RCM uses different physical parametrisations for PBL, microphysics, cumulus,  
 380 radiation, and LSM. This enables many structurally different RCMs to be constructed and tested. In  
 381 NARcliM1.0, 36 WRF RCM configurations were designed, tested, and evaluated (Evans et al. 2014).  
 382 NARcliM2.0 physics testing assesses 78 RCM configurations which are progressively tested via three  
 383 phases, where each test phase is informed by the outcomes of the preceding phase to systematically  
 384 remove poor performing RCM options while facilitating the selection of parameterisations that  
 385 perform well during testing. The N=36 RCMs tested for NARcliM1.0 were evaluated based on eight  
 386 representative storm event simulations each of two-weeks duration (Evans et al. 2014). NARcliM2.0  
 387 physics simulations were run over an entire annual cycle (2016) with a two-month spin-up period  
 388 commencing 1 November 2015. Australia experienced a range of weather extremes during 2016  
 389 driven by a range of climatic influences making 2016 a suitable target year (Bureau of Meteorology,  
 390 2017). Whilst assessing RCMs for an entire year improves on assessing for discrete storm events as

391 per physics testing for NARClIM1.0, it was not feasible to run a large RCM physics ensemble for a  
 392 longer duration. Initial and boundary conditions for all phases of the NARClIM2.0 RCM physics test  
 393 simulations were derived from the ERA-Interim reanalysis data set (Dee et al., 2011). ERA-Interim  
 394 was used because ERA5 was not available at the time. The three phases of NARClIM2.0 physics  
 395 testing are as follows:

#### 396 **4.3.1 Phase I (N=36)**

397 Thirty-six RCMs were evaluated in Phase I. One radiation scheme (RRTMG) was tested for both long  
 398 and short-wave radiation (it was held fixed for all RCMs), whereas physics settings for PBL,  
 399 microphysics, cumulus, and LSM were varied. Of the 36 simulations, 18 used the Noah-Unified LSM,  
 400 whilst the remainder used Community Land Model version 4.0 (CLM4). The physics options tested  
 401 are listed in Table 3, where these were selected based on literature review. Each physics test  
 402 simulation is denoted by a 12-digit identifier which comprises 6 pairs of digits, with each pair  
 403 corresponding to the choice of a specific physics option as specified in the WRF namelist.input file.  
 404 These pairs of digits follow the order: planetary boundary layer (pbl) | cloud microphysics (mp) |  
 405 cumulus convection (cu) | shortwave radiation (sw) | longwave radiation (lw) | LSM (sf) and  
 406 correspond to the WRF namelist options shown in Table 3. For example, the simulation  
 407 050601040402 is interpreted as: 05 | 06 | 01 | 04 | 04 | 02 and denotes that this simulation uses the  
 408 following physics settings:

bl\_pbl\_physics = 05 (MYNN2)  
 mp\_physics = 06 (WSM6)  
 cu\_physics = 01 (Kain-Fritsch)  
 ra\_sw\_physics = 04 (RRTMG)  
 ra\_lw\_physics = 04 (RRTMG)  
 sf\_surface\_physics = 02 (Noah Unified)

409 The complete set of WRF RCM configurations tested in Phase I is shown in Supporting Information  
 410 Table S2.

411 **Table 3.** Physics options used in phase I (N=36) tests.

| Physics Option Description | WRF Namelist   | Options Tested    | Reference                |
|----------------------------|----------------|-------------------|--------------------------|
| Planetary boundary layer   | bl_pbl_physics | 01 = YSU          | Hong et al. (2006)       |
|                            |                | 05 = MYNN2        | Nakanishi & Niino (2009) |
|                            |                | 07 = ACM2         | Pleim (2007)             |
| Microphysics               | mp_physics     | 06 = WSM6         | Hong and Lim (2006)      |
|                            |                | 08 = Thompson     | Thompson et al. (2008)   |
| Cumulus parameterisation   | cu_physics     | 01 = Kain-Fritsch | Kain (2004)              |
|                            |                | 02 = BMJ          | Janjić (2000)            |
|                            |                | 06 = Tiedtke      | Tiedtke (1989)           |



|                     |                    |   |  |
|---------------------|--------------------|---|--|
| Shortwave radiation | ra_sw_physics      | 04 = RRTMG  | Iacono et al. (2008)                         |
| Longwave radiation  | ra_lw_physics      | 04 = RRTMG  |  |
| Land surface model  | sf_surface_physics | 02 = Noah-Unified<br>05 = Community Land Model V4 | Tewari et al. (2016)<br>Oleson et al. (2010) |

412 **4.3.2 Phase II (N=60): additional LSM and radiation scheme tests**

413 Phase I RCMs using CLM4.0 were omitted from further testing because they did not consistently im-  
414 prove performance in simulating the Australian climate relative to RCMs using Noah-Unified. In ad-  
415 dition, RCMs using CLM4.0 had increased simulation times (by approximately twice when compared  
416 to Noah-Unified). Hence, Phase II focused exclusively on further testing of the RCM configurations  
417 that used the Noah-Unified LSM.

418 The physics settings tested in Phase II are an alternative LSM to Noah-Unified (Noah Multi-  
419 Parameterisation; Noah-MP, Niu et al., 2011) and New Goddard radiation (Chou et al., 2001). Owing  
420 to time/resource constraints, testing all eighteen Phase I RCMs using Noah-Unified was not feasible.  
421 To reduce the number of RCMs for further testing, the worst-performing Noah-Unified based RCM  
422 configurations identified in Phase I were excluded. The N=18 RCMs using Noah-Unified are listed  
423 along with their overall performance total scores in Table 4 where the lowest scores under Rank totals  
424 indicate the RCMs that overall perform relatively well versus their peers (see Sect. 3 Evaluation  
425 Methods). Note that the Overall rank denotes the RCMs' relative ranking among all Phase I RCMs.  
426 There is a sharp reduction in rank totals for RCMs #13-18 inclusive, relative to RCMs #1-12. There-  
427 fore, RCMs #13-18 are excluded from further testing, and RCMs #1-12 are retained.

428 **Table 4.** RCM physics combination ranks of the Phase I, N=18 Noah Unified (NU) based RCMs.  
429 Scores/ranks are based on model bias and root mean square error for annual and seasonal precipita-  
430 tion, minimum temperature, maximum temperature, climate extremes (wettest and hottest days), and  
431 Perkins Skill Scores (see Sect. 3). RCMs #1-12 are selected for further testing.

| RCM # | RCM ID       | Physics combination |          |         |       |     | Rank total | Overall rank in N=36 Phase I |
|-------|--------------|---------------------|----------|---------|-------|-----|------------|------------------------------|
|       |              | PBL                 | MP       | Cumulus | SW/LW | LSM |            |                              |
| 1     | 070801040402 | ACM2                | Thom     | KF      | RRTMG | NU  | 484        | 1                            |
| 2     | 070601040402 | ACM3                | WSM6     | KF      | RRTMG | NU  | 495        | 2                            |
| 3     | 070802040402 | ACM4                | Thom     | BMJ     | RRTMG | NU  | 527        | 3                            |
| 4     | 070602040402 | ACM5                | WSM6     | BMJ     | RRTMG | NU  | 559        | 4                            |
| 5     | 010802040402 | YSU                 | Thom     | BMJ     | RRTMG | NU  | 574        | 7                            |
| 6     | 050801040402 | MYNN2               | Thom     | KF      | RRTMG | NU  | 583        | 8                            |
| 7     | 010801040402 | YSU                 | Thompson | KF      | RRTMG | NU  | 617        | 11                           |
| 8     | 050802040402 | MYNN2               | Thompson | BMJ     | RRTMG | NU  | 630        | 12                           |

|    |              |       |          |         |       |    |     |    |
|----|--------------|-------|----------|---------|-------|----|-----|----|
| 9  | 070606040402 | ACM2  | WSM6     | Tiedtke | RRTMG | NU | 639 | 13 |
| 10 | 050601040402 | MYNN2 | WSM6     | KF      | RRTMG | NU | 662 | 16 |
| 11 | 070806040402 | ACM2  | Thompson | Tiedtke | RRTMG | NU | 662 | 16 |
| 12 | 010602040402 | YSU   | WSM6     | BMJ     | RRTMG | NU | 674 | 19 |
| 13 | 010601040402 | YSU   | WSM6     | KF      | RRTMG | NU | 702 | 23 |
| 14 | 010606040402 | YSU   | WSM6     | Tiedtke | RRTMG | NU | 759 | 25 |
| 15 | 050606040402 | MYNN2 | WSM6     | Tiedtke | RRTMG | NU | 766 | 27 |
| 16 | 050602040402 | MYNN2 | WSM6     | BMJ     | RRTMG | NU | 811 | 31 |
| 17 | 010806040402 | YSU   | Thompson | Tiedtke | RRTMG | NU | 830 | 34 |
| 18 | 050806040402 | MYNN2 | Thompson | Tiedtke | RRTMG | NU | 857 | 35 |

432 This gives two sets of physics combinations for additional testing: 1) one replaces only RRTMG  
433 (|04|04|) for short and longwave radiation with New Goddard (|05|05|) making no other changes; and  
434 2) RRTMG radiation is retained, but Noah-MP (|04|) replaces Noah-Unified (|02|). This creates an ad-  
435 ditional 24 RCM configurations for assessment, bringing the total RCMs tested to 60. Although  
436 Noah-MP has several parameter options, Phase II uses its default settings.

#### 437 **4.3.3 Phase III (N=78): parameterising Noah-MP**

438 Phase II shows that RCM performance using New Goddard radiation is generally inferior to the same  
439 RCMs using RRTMG (see Sect. 5. RCM Physics test results). Consequently, RRTMG radiation is re-  
440 adopted for Phase III. Conversely, a general performance improvement is conferred by using Noah-  
441 MP over Noah-Unified (Sect. 5). Given this performance improvement using Noah-MP with default  
442 settings, Phase III assesses RCM performances using specific parameter settings for Noah-MP.

443 Noah-MP provides a dynamic vegetation cover model option (referred to as dynamic vegeta-  
444 tion in the WRF users' guide) (Niu et al., 2011). When deactivated (the default), monthly leaf area in-  
445 dex (LAI) is prescribed for various vegetation types and the greenness vegetation fraction (GVF)  
446 comes from monthly GVF climatological values. Conversely, when dynamic vegetation cover is acti-  
447 vated, LAI and GVF are calculated using a dynamic leaf model. We clarify here that dominant plant-  
448 functional types do not change when using this option, but only the LAI and GVF, i.e., only the  
449 amount of green cover changes.

450 Noah-MP also provides several options for modelling surface run-off and groundwater pro-  
451 cesses including a TOPMODEL (TOPography based hydrological MODEL)-based surface runoff  
452 scheme and a simple groundwater model (SIMGM; Niu et al., 2011). Some studies have shown that  
453 using this option improves the modelling of soil moisture (e.g. Zhuo et al., 2019). Thus, three new sets  
454 of physics configurations are tested using Noah-MP where default options for specific settings are  
455 changed as follows:

- 456 4. activate dynamic vegetation cover (dveg=2 in the WRF namelist); no other changes.
- 457 5. activate TOPMODEL runoff with simple groundwater (opt\_run=1); no other changes.

458 6. activate both dynamic vegetation and TOPMODEL runoff with simple groundwater; no other  
 459 changes.

460 As above, the worst performing RCMs in Phase II are excluded from Phase III testing. Based  
 461 on the RCM configuration performance rankings (Table 5), there is a sharp reduction in performance  
 462 starting from RCM #7 inclusive. Therefore, RCMs #7-12 are excluded from further testing. Phase III  
 463 thus comprises 18 new test simulations (sets 1-3 each comprising 6 RCMs) bringing the total RCMs  
 464 tested to N=78. Phase III physics tests are denoted using the same RCM identification schemes distin-  
 465 guished by appending set\_1, set\_2, set\_3 to identifiers.

466 **Table 5.** RCM physics combination ranks of the Phase II Noah-MP RCMs. Scores/ranks are based on model  
 467 bias and root mean square error for annual and seasonal precipitation, minimum temperature, maximum temper-  
 468 ature, climate extremes (wettest and hottest days), and Perkins Skill Scores (see Sect. 3).

| No. | Physics combination | Rank total |
|-----|---------------------|------------|
| 1   | 50801040404         | 721        |
| 2   | 70806040404         | 822        |
| 3   | 50802040404         | 848        |
| 4   | 70802040404         | 872        |
| 5   | 70601040404         | 880        |
| 6   | 50601040404         | 891        |
| 7   | 10802040404         | 988        |
| 8   | 70602040404         | 1005       |
| 9   | 70606040404         | 1028       |
| 10  | 10801040404         | 1042       |
| 11  | 70801040404         | 1056       |
| 12  | 10602040404         | 1264       |

#### 469 **4.3.4 Shortlisting Physics Test RCMs for ERA5-NARClIM2.0 evaluation simulations**

470 Considering the complete NARClIM2.0 N=78 physics test ensemble, to identify physics test RCMs  
 471 that perform poorly overall, RCMs are eliminated if they are in the lowest 1/3 for RCM performance  
 472 ranks for any of maximum temperature, minimum temperature, precipitation, or for the overall model  
 473 performance rank across these variables (see Sect. 5. RCM Physics test results). Under this scheme,  
 474 20 RCMs remain. The independence measures are then applied to the remaining 20 RCMs to choose a  
 475 final subset of 7 RCMs for ERA5-forced evaluation simulations (see Sect. 4.4). The ensemble size  
 476 limit of N=7 is determined by available compute resources. These 7 candidate RCMs are assessed for  
 477 potential use in the CMIP6 GCM-forced downscaling phase of NARClIM2.0 (Sect. 4.4 and Di Vir-  
 478 gilio et al. 2024).

#### 479 **4.4 CORDEX ERA5-NARClIM2.0 evaluation simulations**

480 NARClIM1.x performed production climate simulations using a two-phase process. Its RCM physics  
481 testing selected definitive production-grade RCMs which were then used to downscale both reanalysis  
482 data and CMIP3/5 GCMs. In contrast, for NARClIM2.0, as described above the N=78 RCM physics  
483 testing culminates in shortlisting 7 production-candidate RCMs which are used to downscale the  
484 ERA5 reanalysis for 42-years (1979-2020). This enables assessment of the performances of these 7  
485 shortlisted RCMs over a climatological period rather than the single year (2016) of the physics test-  
486 ing, which helps ascertain that performance differences between shortlisted RCMs are robust across a  
487 multi-decadal timescale capturing climatologically diverse years. The aim is that two definitive pro-  
488 duction-grade RCMs can be selected for CMIP6-forced downscaling from these ERA5-forced  
489 CORDEX evaluation simulations. Thus, the seven ERA5-NARClIM2.0 RCMs were driven by  
490 ERA5.0 boundary conditions for January 1979 to December 2020 using the model and nested domain  
491 setups described above for NARClIM2.0. The skill of these RCMs in simulating the recent Australian  
492 climate was assessed as follows (see Di Virgilio et al. 2024): annual and seasonal means were calcu-  
493 lated for maximum and minimum temperature and precipitation using monthly means for temperature  
494 variables, and the monthly sum for precipitation. Extremes of maximum temperature and precipitation  
495 (99<sup>th</sup> percentiles) and extreme minimum temperature (1<sup>st</sup> percentile) were calculated using daily data.  
496 RCM performances in reproducing observations over these timescales were assessed by calculating  
497 model outputs minus observations (i.e., model bias), and the RMSE of modelled versus observed  
498 fields. RCM skill in simulating distributions of observed variables was assessed by comparing the  
499 PDFs for daily mean observations versus those of the RCMs. The ultimate outcome of these ERA5-  
500 forced simulations and their evaluation is the selection of two definitive RCM configurations, R3 and  
501 R5, to run the CMIP6-forced phase of NARClIM2.0, see Di Virgilio et al. (2024) for further details on  
502 the evaluation methods and results. Supporting Information Figure S1 shows the WRF namelist set-  
503 tings for the R3 and R5 RCMs (see also Sect. 9. Code Availability).

#### 504 **4.5 CORDEX CMIP6-forced NARClIM2.0 simulations**

505 The ideal CMIP6 GCM variables and their frequencies required to run the WRF RCM are listed in  
506 Table S1. A minority of variables in Table S1 are not available at sub-daily frequencies for every tar-  
507 get GCM. This necessitates assumptions/data proxies to be made. For instance, soil moisture and soil  
508 temperature variables were unavailable for some selected GCMs; hence, surrogate data, such as sur-  
509 face temperature, were used for initialisation (noting that soil data are only used by the RCM at ini-  
510 tialisation). In these cases, we investigated how long it took for uncertainty in the initial conditions to  
511 disappear from the WRF output by analysing the regionally averaged soil moisture time series. The  
512 data were regionalised according to the four Australian Natural Resource Management (NRM)

513 regions / climate zones (Supporting Information Figure S2) which are broadly aligned with climato-  
514 logical boundaries (Fiddes et al., 2021) and with the IPCC reference regions (Iturbide et al., 2020).  
515 Time series plots (Figure S3) show that soil moisture equilibrates to be within a normal range follow-  
516 ing initialisation, indicating that the 12-month spin-up year (1950) is sufficient to account for the as-  
517 sumptions made at model initialisation.

518 Boundary and initial conditions were prepared using selected GCM data to run the 151-year  
519 GCM-driven simulations using WRF version 4.1.2. The GCM-driven simulations were run and com-  
520 pleted using the pre-defined RCM settings for the two definitive RCM configurations using the WRF  
521 namelists in Supporting Information Figure S1 (see also Sect. 9. Code Availability). A cold restart  
522 was performed on the last Historical experiment year (2014), thus enabling the SSP1-2.6 and SSP3-  
523 7.0 experiments to be run for 2015-2100 concurrently with the Historical experiment. Testing the time  
524 duration required for soil moisture to equilibrate from the cold start showed that 1 year is sufficient.  
525 The 2014 cold start year is eventually overwritten by Historical runs initiated in 1950.

## 526 **5. RCM Physics test results**

### 527 **5.1 Phase I RCM performance summary**

528 The spatial variation and magnitudes for Phase I RCM biases and RMSEs for annual mean maximum  
529 and minimum temperature and precipitation are shown in Figures 4-5, respectively. Overall, RCMs  
530 are biased cold for maximum temperature (mean absolute bias for the ensemble mean = 1.18 K), and  
531 warm-biased for minimum temperature (mean absolute bias = 1.31 K; Figure 4a-b). Maximum tem-  
532 perature RMSE magnitudes are large over the elevated terrain of the southeast coast and over western  
533 regions (Figure 5a). The simulation of precipitation shows biases of varying sign, with wet biases that  
534 are strongest over eastern coastal regions (Figure 4c). Precipitation RMSEs are particularly large  
535 along the eastern coastline (>15 mm), and generally show an east-west gradient, i.e., progressively  
536 decreasing further inland from the coast (Figure 5c).

### 537 **5.2 Comparing Phase II Physics Test RCM performances versus Phase I**

#### 538 **5.2.1 Climate Means**

539 Overall, the RCM ensemble using New Goddard (NG) radiation has inferior performance to the corre-  
540 sponding RCMs using RRTMG in terms of annual/seasonal mean maximum temperature biases,  
541 RMSEs, and PSS (Table 7). In contrast, NG confers superior performance for annual/seasonal mean  
542 minimum temperature for these statistics. RCMs using NG show reduced biases for annual mean and  
543 spring-time precipitation, but larger errors for DJF and JJA (Table 7). RMSEs for annual and seasonal  
544 precipitation are similarly variable.

545 **Table 7.** Climate means performance: phase II physics tests (i.e., N=12 set 1 changing only RRTMG to New  
546 Goddard (NG) and N=12 set 2 changing only land surface model (LSM) from Noah-Unified to Noah-MP  
547 (NMP) compared with the phase I physics test RCMs that were shortlisted for further testing (N=12).

| Variable              | Timescale | Bias                         |                                  |                                  | RMSE                         |                                  |                                  | PSS                          |                                  |                                  |
|-----------------------|-----------|------------------------------|----------------------------------|----------------------------------|------------------------------|----------------------------------|----------------------------------|------------------------------|----------------------------------|----------------------------------|
|                       |           | Phase I (N=12) ensemble mean | Phase II (NG rad.) ensemble mean | Phase II (NMP LSM) ensemble mean | Phase I (N=12) ensemble mean | Phase II (NG rad.) ensemble mean | Phase II (NMP LSM) ensemble mean | Phase I (N=12) ensemble mean | Phase II (NG rad.) ensemble mean | Phase II (NMP LSM) ensemble mean |
| <b>Temp. Max. (K)</b> | Annual    | 0.87                         | 1.27                             | 0.58                             | 3.56                         | 3.73                             | 3.50                             | <b>0.950</b>                 | <b>0.936</b>                     | <b>0.955</b>                     |
|                       | DJF       | 0.74                         | 1.29                             | 0.63                             | 4.41                         | 4.70                             | 4.43                             |                              |                                  |                                  |
|                       | MAM       | 1.40                         | 2.06                             | 0.83                             | 3.68                         | 3.92                             | 3.55                             | -                            | -                                | -                                |
|                       | JJA       | 0.62                         | 0.81                             | 0.52                             | 2.64                         | 2.66                             | 2.65                             |                              |                                  |                                  |
|                       | SON       | 0.87                         | 1.04                             | 0.66                             | 3.25                         | 3.32                             | 3.20                             |                              |                                  |                                  |
| <b>Temp. Min. (K)</b> | Annual    | 1.35                         | 0.95                             | 1.2                              | 3.53                         | 3.41                             | 3.42                             | <b>0.927</b>                 | <b>0.941</b>                     | <b>0.931</b>                     |
|                       | DJF       | 1.50                         | 1.08                             | 0.87                             | 3.86                         | 3.82                             | 3.66                             |                              |                                  |                                  |
|                       | MAM       | 1.21                         | 0.84                             | 0.92                             | 3.55                         | 3.45                             | 3.50                             | -                            | -                                | -                                |
|                       | JJA       | 0.82                         | 0.51                             | 0.91                             | 3.00                         | 2.92                             | 3.00                             |                              |                                  |                                  |
|                       | SON       | 1.88                         | 1.47                             | 1.92                             | 3.63                         | 3.40                             | 3.58                             |                              |                                  |                                  |
| <b>Prec. (mm)</b>     | Annual    | 0.25                         | 0.24                             | 0.25                             | 7.21                         | 7.32                             | 6.78                             | <b>0.943</b>                 | <b>0.950</b>                     | <b>0.946</b>                     |
|                       | DJF       | 0.41                         | 0.53                             | 0.49                             | 8.28                         | 8.83                             | 8.85                             |                              |                                  |                                  |
|                       | MAM       | 0.32                         | 0.32                             | 0.25                             | 5.91                         | 6.47                             | 5.53                             | -                            | -                                | -                                |
|                       | JJA       | 0.37                         | 0.53                             | 0.44                             | 7.63                         | 7.34                             | 7.65                             |                              |                                  |                                  |
|                       | SON       | 0.34                         | 0.22                             | 0.39                             | 6.68                         | 6.18                             | 6.92                             |                              |                                  |                                  |

548 Phase II RCMs using Noah-MP with RRTMG retained show improved performance in simu-  
549 lating mean maximum and minimum temperature at annual timescales and most seasons relative to  
550 corresponding Phase I RCMs using Noah-Unified (Table 7; Figure 4-5). For instance, the mean abso-  
551 lute bias for annual mean maximum temperature is 0.58 K for the Noah-MP ensemble mean versus  
552 1.18 K for the Noah-Unified ensemble. In particular, cold bias magnitudes for maximum temperature  
553 are considerably lower over eastern and southern regions for the RCMs using Noah-MP (Figure 4d).  
554 RMSE magnitudes for maximum temperature are substantially reduced over the topographically com-  
555 plex regions of the southeast, and southwest and central regions (Figure 5d).

556 Overall, the magnitude of warm biases for minimum temperature are broadly similar for  
557 Phase I and Phase II RCMs (Figure 4b,c). Conversely, while RCMs in both Phases show large  
558 RMSEs for minimum temperature over several eastern regions, RMSEs are smaller for the Noah-MP  
559 ensemble over some southern areas (Figure 5b,c).

560 In contrast to the above results for the simulation of maximum temperature, overall, Phase II  
 561 RCMs using Noah-MP show smaller performance improvements for the simulation of precipitation  
 562 relative to the Phase I RCMs (Table 7). However, precipitation bias magnitudes are smaller for the  
 563 Noah-MP ensemble over specific regions, e.g., north-eastern coastal regions and the elevated terrain  
 564 of the south-east (Figure 4c,f).

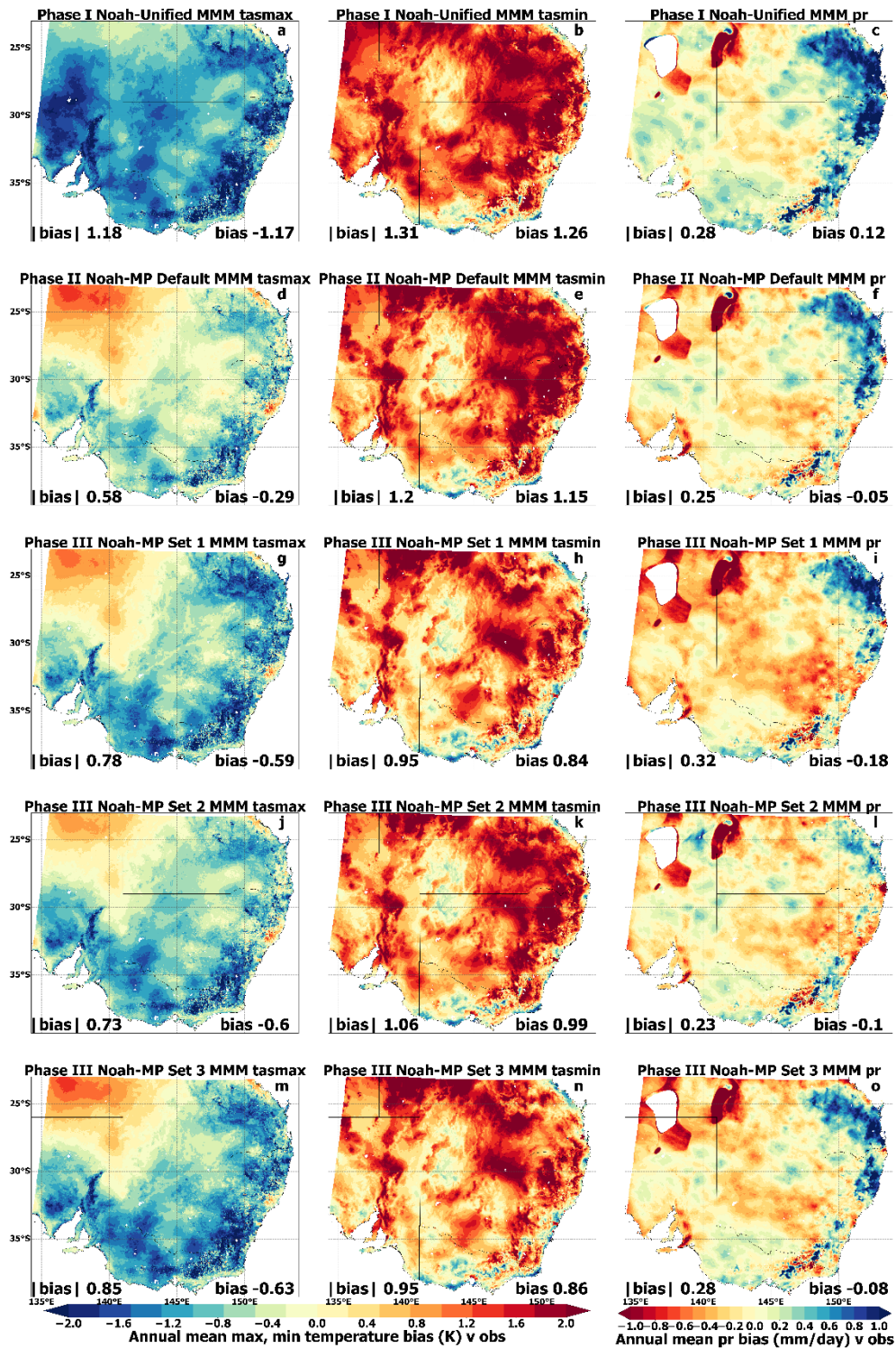
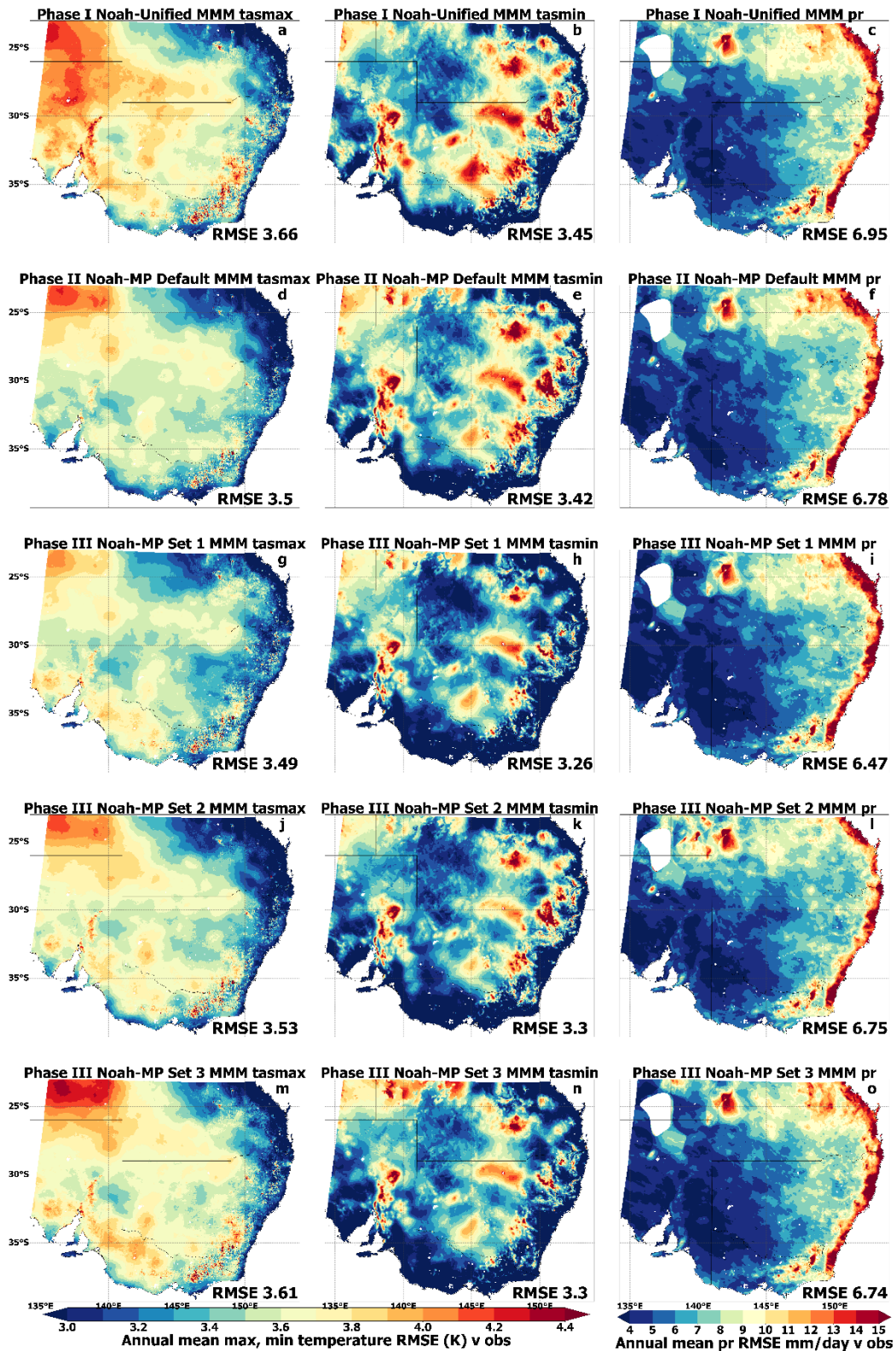


**Figure 4.** Phase I (N=36), Phase II (N=60) and Phase III (N=78) ensemble mean biases for annual mean maximum temperature, minimum temperature and precipitation with respect to Australian Gridded Climate Data

568 (AGCD) observations for NARClm2.0 Phase I physics test RCMs using Noah-Unified as the land surface  
 569 model (LSM) (a-c); Phase II physics test RCMs using Noah-MP as the LSM and its default settings (d-f); Phase  
 570 III set 1 physics test RCMs using Noah-MP with dynamic vegetation cover activated (g-i); Phase III set 2 phys-  
 571 ics test RCMs using Noah-MP with TOPMODEL surface runoff and simple groundwater activated (j-l); and  
 572 Phase III set 3 physics test RCMs using Noah-MP with both dynamic vegetation cover and TOPMODEL runoff  
 573 activated (m-o).



574



575 **Figure 5.** As per Figure 4 but showing RMSEs.

### 576 **5.2.2. Climate Extremes**

577 Climate extreme analysis assesses RCM representations of the hottest and the wettest day versus  
 578 AGCD. For both extremes and for RCM biases and RMSEs, Phase II RCMs using NG radiation  
 579 showed inferior performance relative to phase I RCMs using RRTMG (Table 8). Conversely, Phase II  
 580 RCMs using Noah-MP show substantial reductions in bias for both the hottest and wettest days (Table  
 581 8). Phase II Noah-MP RCMs show a small increase in RMSE for the hottest day (Phase I bias=3.59  
 582 K; Phase II bias=3.74 K); however, RMSEs are smaller for the wettest day (i.e., Phase I RMSE=19.20  
 583 mm; Phase II RMSE=18.47 mm) (Table 8).

584 **Table 8** Climate extremes performance: comparing phase I RCMs (N=12) with phase II RCMs (i.e.,  
 585 12 RCMs changing radiation from RRTMG to New Goddard (NG) and 12 RCMs changing land sur-  
 586 face model (LSM) from Noah-Unified to Noah-MP; NMP).

| Variable                  | Bias                                  |  |  | RMSE                                  |  |  |
|---------------------------|---------------------------------------|--|--|---------------------------------------|--|--|
|                           | Phase I<br>(N=12)<br>ensemble<br>mean | Phase II<br>(NG<br>rad.) en-<br>semble<br>mean | Phase II<br>(NMP<br>LSM)<br>ensemble<br>mean | Phase I<br>(N=12)<br>ensemble<br>mean | Phase II<br>(NG<br>rad.) en-<br>semble<br>mean | Phase II<br>(NMP<br>LSM)<br>ensemble<br>mean |
| Temp. max: hottest<br>(K) | 1.11                                  | 1.93   | 0.81   | 3.59                                  | 3.97   | 3.74   |
| Prec.: wettest<br>(mm)    | 3.08                                  | 3.21   | 2.60   | 19.20                                 | 20.52  | 18.47  |

### 587 **5.3 Phase III RCM performance summary and shortlisting N=7 RCMs for** 588 **ERA5-NARClIM2.0 evaluation simulations**

589 Overall, RCM biases for mean maximum temperature do not show marked improvements once the  
 590 dynamic vegetation cover and surface runoff options are activated for Noah-MP (Figure 4 g,j,m) rela-  
 591 tive to RCMs using Noah-MP with default settings (Figure 4d). However, specifically for the RCM  
 592 ensemble with dynamic vegetation cover activated for Noah-MP, RMSE magnitudes for maximum  
 593 temperature are lower over some eastern coastal regions (Figure 5g).

594 The simulation of mean minimum temperature shows clear performance improvements for  
 595 Phase III RCMs using options activated for Noah-MP, relative to RCMs using Noah-MP defaults.  
 596 Overall, both biases and RMSEs for minimum temperature are reduced in magnitude for RCMs using  
 597 either or both of dynamic vegetation cover and runoff/groundwater options activated for Noah-MP,

598 relative to the default parameters (Figure 4-5). These performance improvements are largest over east-  
599 ern and southern regions.

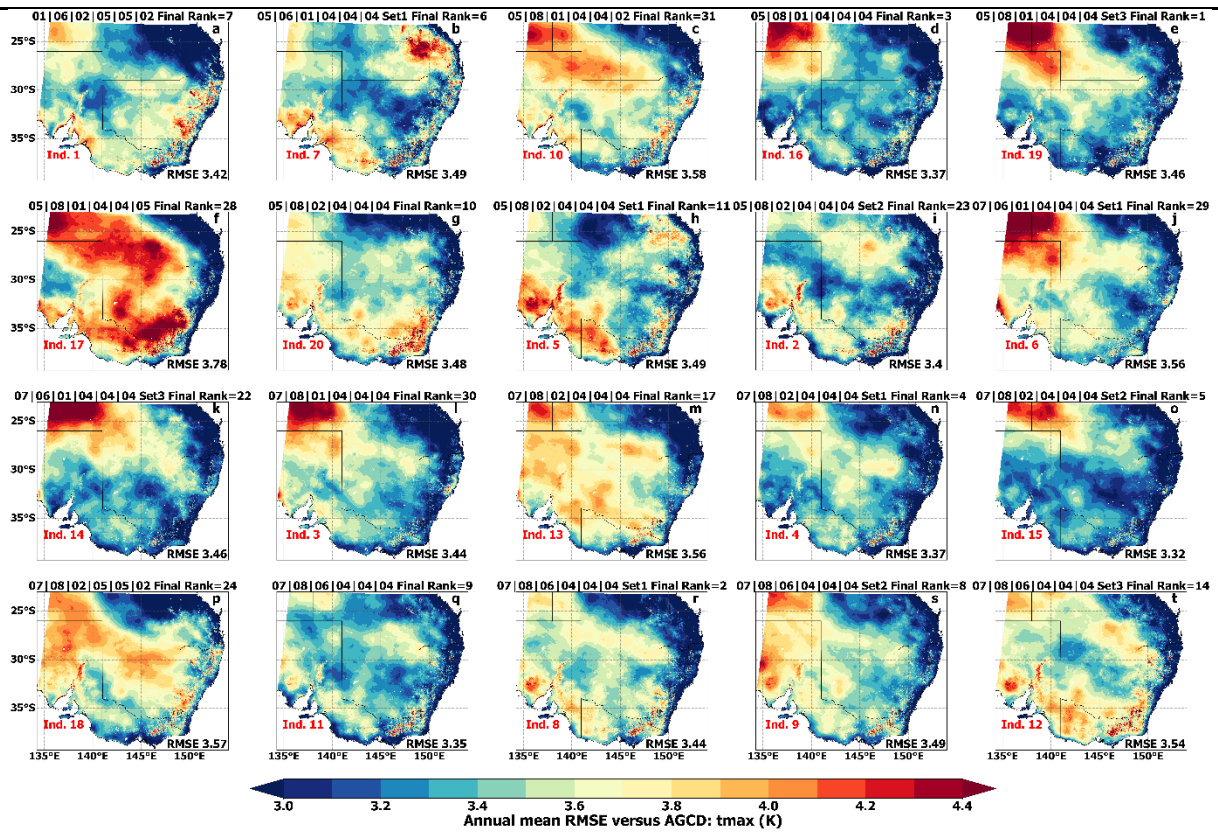
600 There are no substantial overall performance improvements in the simulation of precipitation  
601 for Phase III RCMs relative to Phase II RCMs (Figures 4-5 f,i,l,o). However, using Noah-MP with  
602 specific LSM options remains favourable to using RCMs with Noah-Unified, albeit the performance  
603 gains are generally small, except for some coastal regions and especially the north-east.

604 All 78 RCMs in the complete RCM physics test ensemble are ranked for performance as de-  
605 scribed in Sect. 3.2. Once the poor-performing RCMs are excluded, there are 20 RCMs remaining  
606 (Table 9; Figures 6-8). In Table 9, we see that 16 Noah-MP-based RCMs from Phase II and Phase III  
607 comprise this set of 20 RCMs, with 3 of the 20 RCMs using Noah-Unified, and 1 using CLM4.0. For  
608 maximum temperature, some shortlisted RCMs show substantial RMSEs over north-western and in-  
609 land areas (e.g., Figure 6 d-f) that are of larger magnitude over these areas than the ensemble means of  
610 Phase I-III RCMs (Figure 5). Conversely, several shortlisted RCMs show very low RMSEs for maxi-  
611 mum temperature across eastern and southern regions, especially along the eastern coast (Figure 6,  
612 e.g., RCMs in panels d,l,n,o,q). For minimum temperature, a subset of the twenty shortlisted RCMs  
613 show substantially reduced RMSEs over many regions relative to the Phase I-III ensemble means  
614 (Figure 7, e.g., RCMs in panels: b,h,i). Additionally, several shortlisted RCMs show reduced RMSEs  
615 for precipitation over the eastern coast and north-east (Figure 8, e.g., RCMs in panels: c, l, m, n, o)  
616 relative to the Phase I-III RCM ensemble means in Figure 5c,f,i,l,o.

617 These 20 RCMs are assessed for statistical independence and 7 RCMs from this RCM set are  
618 shortlisted for the ERA5-forced RCM simulations considering both their performance and independ-  
619 ence scores (Table 9). These 7 shortlisted RCMs are listed in **bold** in Table 9 and are identified as R1-  
620 R7 in the ERA5-forced evaluation simulations (Table 9; final column). RCMs are shortlisted from the  
621 set of 20 if they rank highly for both performance and independence. For instance, RCM  
622 050801040404\_set\_3 (top row, Table 9) is top-ranked for performance, however, its independence  
623 scores/ranks are low, hence it is not shortlisted. It is important to note that, while a general perfor-  
624 mance gain is observed in the physics testing when using Noah-MP, there are some specific RCM  
625 configurations using Noah-Unified that perform well in simulating the Australian climate. For in-  
626 stance, the RCM 010602050502 (row 7; Table 9; R1) uses Noah-Unified and performs well overall  
627 (its overall performance rank=7), and especially for the simulation of maximum temperature (Figure  
628 6a). It is also the only RCM in this set of 20 RCMs to use YSU for PBL. Importantly, this RCM is  
629 highly ranked for statistical independence, hence, this RCM is shortlisted for the N=7 set. We note  
630 here that R1-R7 are simply a chronological naming convention and do not imply any ranking for these  
631 7 RCM configurations.

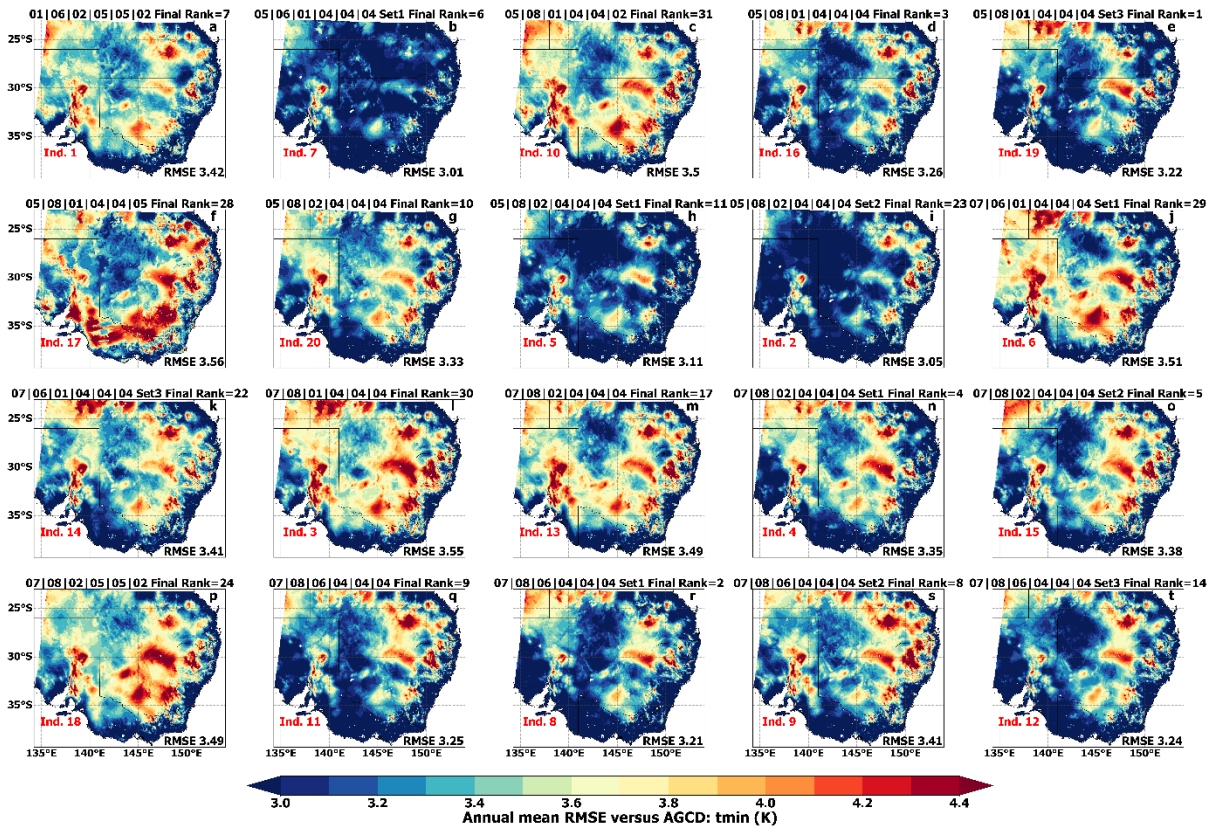
632 **Table 9.** The 20 NARClIM2.0 physics test RCMs shortlisted from the ensemble of 78 RCMs based on their per-  
633 formance in simulating the Australian climate and independence (Ind.). N=7 R1-R7 RCMs shortlisted for  
634 ERA5-forced evaluation simulations shown in **bold**. R1-R7 are a naming convention and do not imply a ranking  
635 for these 7 RCMs. NU=Noah Unified; NMP=Noah-MP; DV=dynamic vegetation cover; TOP=topmodel runoff.

| # | RCM Physics Combination   | PBL          | MP          | Cu- mulus  | SW/LW        | LSM            | Test Phase | Overall Performance Rank | Bishop Abramowitz Ind. Rank | Heger Ind. Set 1 | Heger Ind. Set 2 | ERA5-forced RCM Identifier |
|---|---------------------------|--------------|-------------|------------|--------------|----------------|------------|--------------------------|-----------------------------|------------------|------------------|----------------------------|
| 1 | 050801040404_set_3        | MYNN2        | Thom        | KF         | RRTMG        | NMP DV+TOP     | III        | 1                        | 19                          | 20               | 20               |                            |
| 2 | <b>070806040404_set_1</b> | <b>ACM2</b>  | <b>Thom</b> | <b>Td</b>  | <b>RRTMG</b> | <b>NMP DV</b>  | <b>III</b> | <b>2</b>                 | <b>8</b>                    | <b>5</b>         | <b>6</b>         | <b>R6</b>                  |
| 3 | 50801040404               | MYNN2        | Thom        | KF         | RRTMG        | NMP            | II         | 3                        | 16                          | 12               | 13               |                            |
| 4 | <b>070802040404_set_1</b> | <b>ACM2</b>  | <b>Thom</b> | <b>BMJ</b> | <b>RRTMG</b> | <b>NMP DV</b>  | <b>III</b> | <b>4</b>                 | <b>4</b>                    | <b>3</b>         | <b>3</b>         | <b>R5</b>                  |
| 5 | 070802040404_set_2        | ACM2         | Thom        | BMJ        | RRTMG        | NMP TOP        | III        | 5                        | 15                          | 13               | 12               |                            |
| 6 | <b>050601040404_set_1</b> | <b>MYNN2</b> | <b>WSM6</b> | <b>KF</b>  | <b>RRTMG</b> | <b>NMP DV</b>  | <b>III</b> | <b>6</b>                 | <b>7</b>                    | <b>10</b>        | <b>10</b>        | <b>R2</b>                  |
| 7 | <b>10602050502</b>        | <b>YSU</b>   | <b>WSM6</b> | <b>BMJ</b> | <b>NG</b>    | <b>NU</b>      | <b>II</b>  | <b>7</b>                 | <b>1</b>                    | <b>3</b>         | <b>3</b>         | <b>R1</b>                  |
| 8 | <b>070806040404_set_2</b> | <b>ACM2</b>  | <b>Thom</b> | <b>Td</b>  | <b>RRTMG</b> | <b>NMP TOP</b> | <b>III</b> | <b>8</b>                 | <b>9</b>                    | <b>9</b>         | <b>5</b>         | <b>R7</b>                  |
| 9 | 70806040404               | ACM2         | Thom        | Td         | RRTMG        | NMP            | II         | 9                        | 11                          | 14               | 14               |                            |
| # | 50802040404               | MYNN2        | Thom        | BMJ        | RRTMG        | NMP            | II         | 10                       | 20                          | 19               | 19               |                            |
| # | <b>050802040404_set_1</b> | <b>MYNN2</b> | <b>Thom</b> | <b>BMJ</b> | <b>RRTMG</b> | <b>NMP DV</b>  | <b>III</b> | <b>11</b>                | <b>5</b>                    | <b>2</b>         | <b>2</b>         | <b>R3</b>                  |
| # | 070806040404_set_3        | ACM2         | Thom        | Td         | RRTMG        | NMP DV+TOP     | III        | 14                       | 12                          | 10               | 10               |                            |
| # | 70802040404               | ACM2         | Thom        | BMJ        | RRTMG        | NMP            | II         | 17                       | 13                          | 15               | 15               |                            |
| # | 070601040404_set_3        | ACM2         | WSM6        | KF         | RRTMG        | NMP DV+TOP     | III        | 22                       | 14                          | 16               | 16               |                            |
| # | <b>050802040404_set_2</b> | <b>MYNN2</b> | <b>Thom</b> | <b>BMJ</b> | <b>RRTMG</b> | <b>NMP TOP</b> | <b>III</b> | <b>23</b>                | <b>2</b>                    | <b>4</b>         | <b>4</b>         | <b>R4</b>                  |
| # | 70802050502               | ACM2         | Thom        | BMJ        | NG           | NU             | II         | 24                       | 18                          | 18               | 18               |                            |
| # | 50801040405               | MYNN2        | Thom        | KF         | RRTMG        | CLM4           | I          | 28                       | 17                          | 17               | 17               |                            |
| # | 070601040404_set_1        | ACM2         | WSM6        | KF         | RRTMG        | NMP DV         | III        | 29                       | 6                           | 7                | 8                |                            |
| # | 70801040404               | ACM2         | Thom        | KF         | RRTMG        | NMP            | II         | 30                       | 3                           | 1                | 1                |                            |

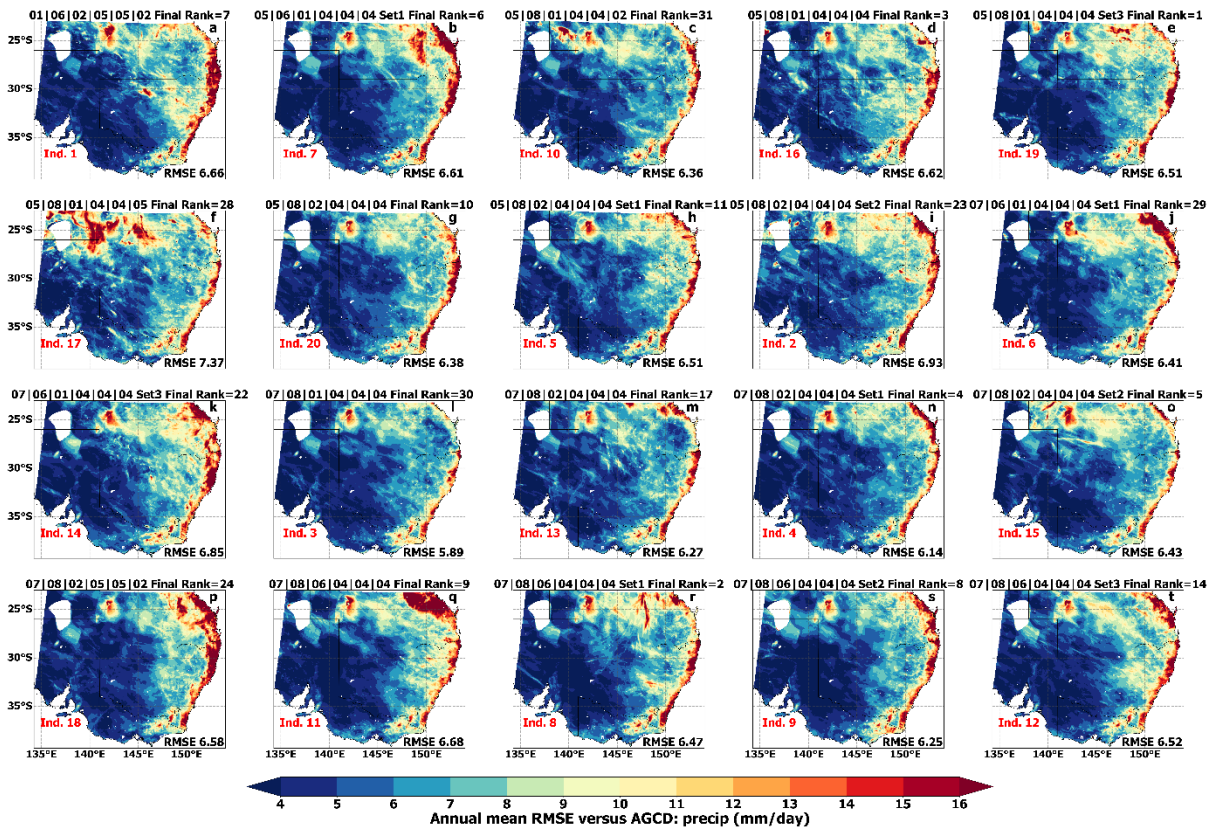


636

637 **Figure 6.** RMSEs for modelled mean maximum temperature (tmax) versus observations for the twenty  
 638 NARClM2.0 physics test RCMs shortlisted from the full ensemble of seventy-eight RCMs based on their  
 639 performance in simulating the recent south-east Australian climate. Overall (final) performance ranks and  
 640 Bishop and Abramowitz (2013) method independence (Ind.) scores are shown.



641  
642 **Figure 7.** As per Figure 6 but for mean minimum temperature (tmin).

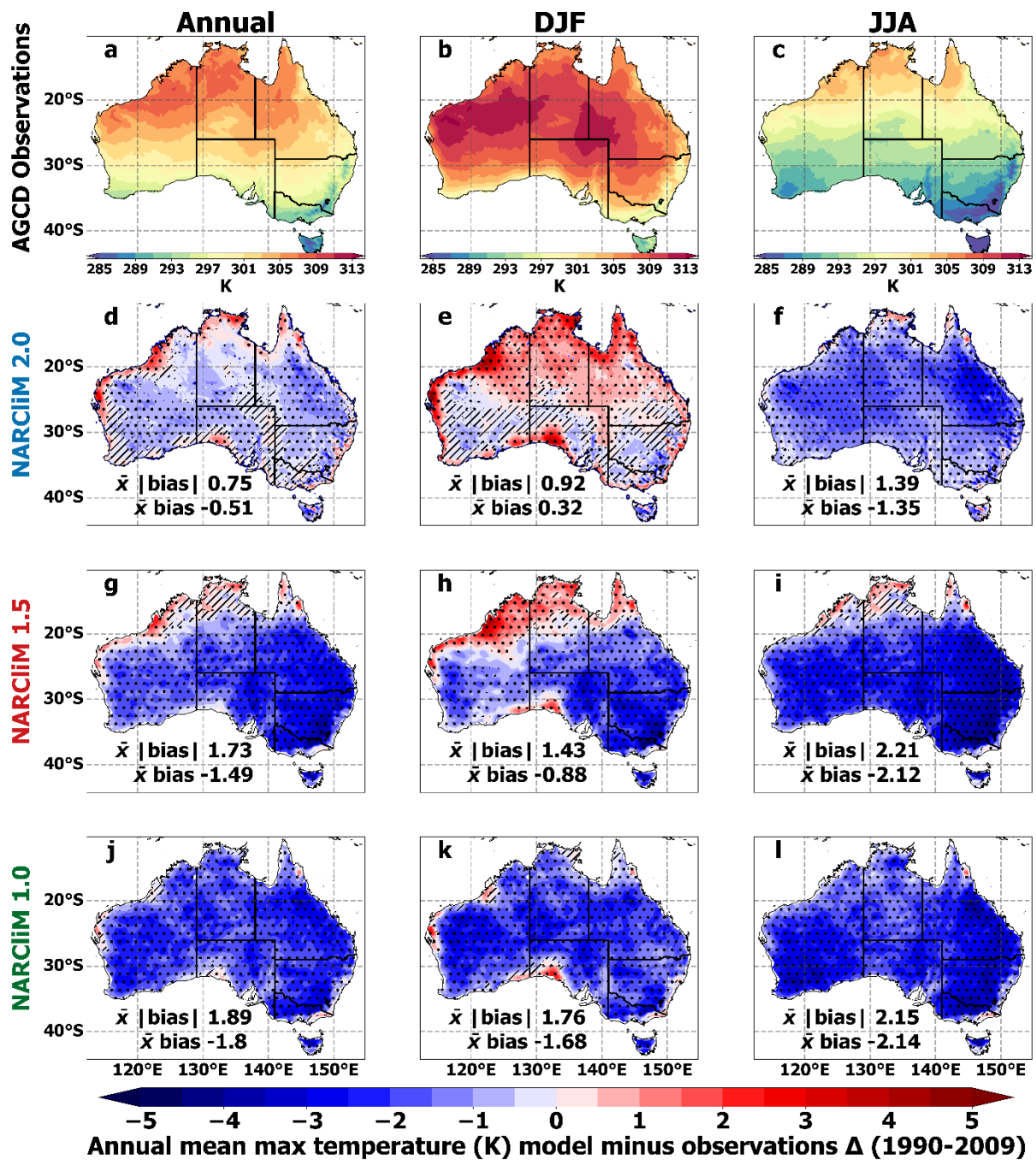


643  
644 **Figure 8.** As per Figure 6 but for mean precipitation (precip.).

## 645 **6. CORDEX-CMIP6 NARClIM2.0 historical evaluation**

### 646 **6.1 Maximum temperature**

647 Overall, NARClIM2.0 RCMs simulate maximum temperature more accurately than NARClIM1.x,  
648 with widespread, statistically significant reductions in cold biases in the ensemble mean (Figure 9), as  
649 well as for many individual RCMs (Supporting Information Figure S4-S6). These reductions in bias  
650 apply for all timescales but are largest for the annual mean, i.e., the area-averaged mean absolute bias  
651 for the NARClIM2.0 ensemble is 0.75 K (range: 0.61 to 2.03 K), 1.73 K (range: 1.1 to 2.37 K) for  
652 NARClIM1.5, and 1.89 K (range: 0.55 to 4.12 K) for NARClIM1.0 (Figure 9d,g,j and Figure S4). No-  
653 tably, the NARClIM2.0 ensemble mean annual mean maximum temperature bias magnitudes are  
654 small, i.e., around  $<0.5$  K, over south-west WA, southern coastal regions, and several eastern regions.  
655 This may be important from a climate change adaptation and mitigation perspective as these regions  
656 are heavily populated and economically significant. NARClIM2.0 retains warm biases of similar mag-  
657 nitude to NARClIM1.5 along the north-west coast of Australia (Figure 9d,g). Moreover, these warm  
658 biases cover additional areas for NARClIM2.0, especially during DJF (Figure 9e,h). A wide range of  
659 bias signs are evident for the individual NARClIM2.0 ensemble members (Figures S4-S6) and a mi-  
660 nority of NARClIM2.0 RCMs retain strong cold biases, e.g., at an annual timescale NARClIM2.0-  
661 NorESM2-MM R3 (mean absolute bias = 2.03 K) and UKESM-1-0-LL R3 (1.77 K). Additionally, the  
662 R5 RCM is generally warmer than R3 (e.g., Figure S4c,d). Considering the forcing GCM data, over-  
663 all, ensemble means for the CMIP6 and CMIP5 GCMs generally show similar patterns and magni-  
664 tudes of cold bias for maximum temperature (Supporting Information S7).



665

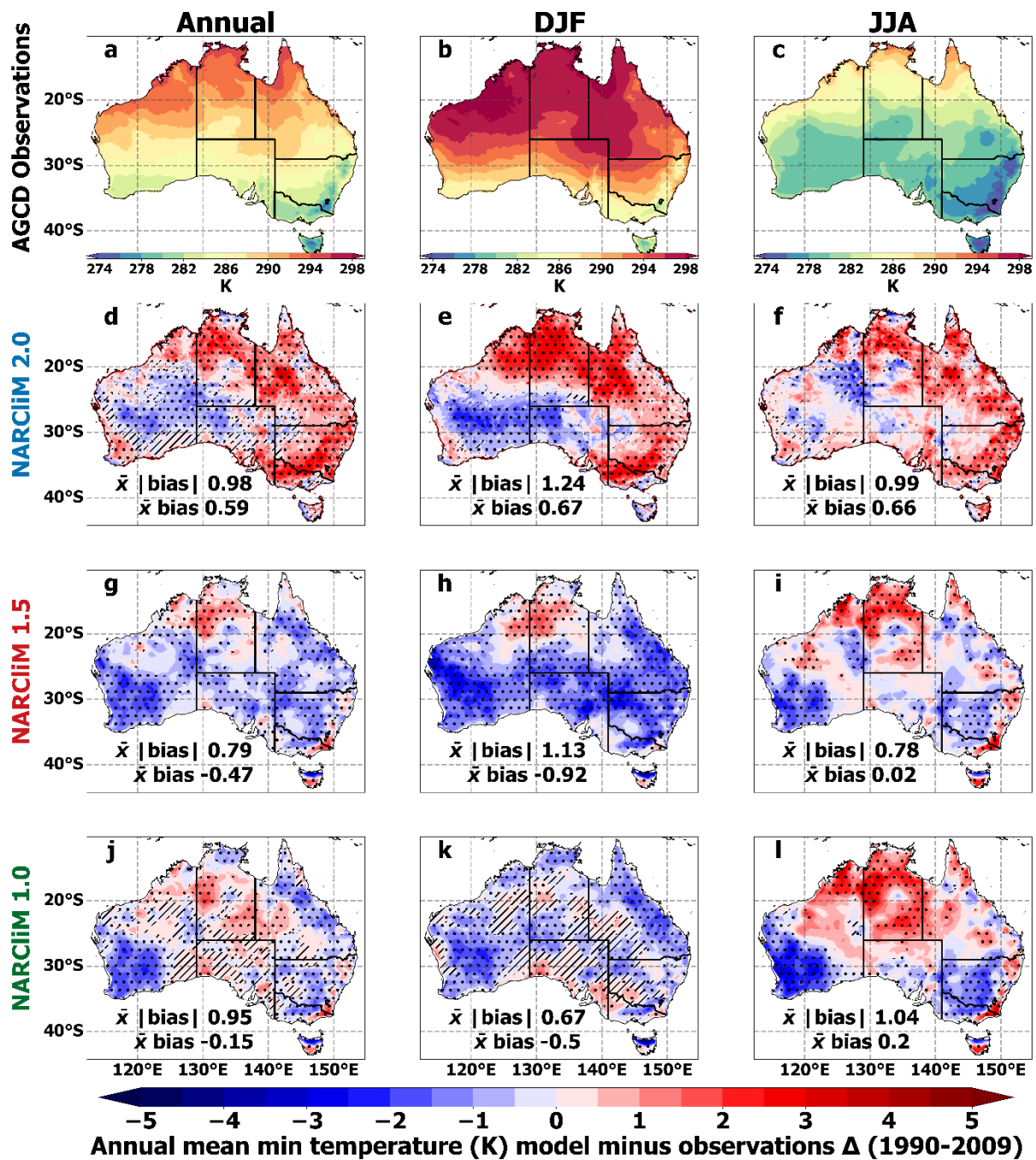
666 **Figure 9.** Annual, DJF and JJA mean near-surface atmospheric maximum temperature biases for NARCIIM2.0,  
 667 1.5 and 1.0 historical ensemble means with respect to Australian Gridded Climate Data (AGCD) observations  
 668 for 1990-2009. Stippled areas indicate locations where an RCM shows statistically significant bias. Significance  
 669 stippling for the ensemble mean bias follows Tebaldi et al. (2011) and is applied separately to each RCM en-  
 670 semble. Statistically insignificant areas are shown in colour, denoting that less than half of the models are signif-  
 671 icantly biased. In significant agreeing areas (stippled), at least half of RCMs are significantly biased, and at least  
 672 70% of significant RCMs in each ensemble agree on the direction of the bias. Significant disagreeing areas are  
 673 shown in hatching, which are where at least half of the models are significantly biased and less than 70% of sig-  
 674 nificant models in each ensemble agree on the bias direction - see main text for additional detail on the stippling  
 675 regime.

## 676 **6.2 Minimum temperature**

677 The simulation of mean minimum temperature by NARClIM2.0 is generally warm biased at all time-  
678 scales (Figure 10). Its bias magnitudes over many regions are larger versus NARClIM1.5, e.g., annual  
679 mean area-averaged absolute biases are 0.98 K and 0.79 K for NARClIM2.0 and NARClIM1.5, re-  
680 spectively (Figure 10 d,g). However, there are exceptions to this result over specific regions, for ex-  
681 ample, parts of south-west western Australia show annual mean bias magnitudes of <1 K for NAR-  
682 ClIM2.0, but these areas show biases below -2 K for NARClIM1.x (Figure 10d,g,j). Most individual  
683 RCMs comprising the NARClIM2.0 ensemble show stronger warm biases than their NARClIM1.5  
684 peers at both annual and seasonal timescales (Figures S8-S10). The ACCESS-ESM-1-5-forced NAR-  
685 ClIM2.0 RCMs are considerably more warm-biased than the other NARClIM2.0 RCMs, with average  
686 absolute biases of 1.74 K and 1.9 K; Fig. S8c-d).

687 Many of the CMIP6 GCMs used to force the NARClIM2.0 RCMs are warmer than the CMIP5  
688 GCMs used to force NARClIM1.5, such that the ensemble mean bias of the former is 1.9 K versus  
689 1.11 K (Figure S11). In particular, ACCESS-ESM-1-5 and MPI-ESM1-2-HR are substantially more  
690 warm-biased relative to all other selected GCMs, with mean absolute biases of 2.2K and 3.47K, re-  
691 spectively (Figure S11). This suggests that NARClIM2.0's warm biases for mean minimum tempera-  
692 ture are at least partially inherited from the driving data. However, whilst the ACCESS-ESM-1-5-  
693 forced NARClIM2.0 RCMs are much warmer than their counterparts (i.e., 1.74 K and 1.9 K), this  
694 does not apply to the MPI-ESM1-2-HR-forced RCMs, which have biases of only 1.01 K and 1.09 K.  
695 Hence, factors additional to the driving data, such as changes in RCM parameterisations between  
696 NARClIM generations and other model design changes likely contribute to the warmer biases ob-  
697 served for NARClIM2.0.





698

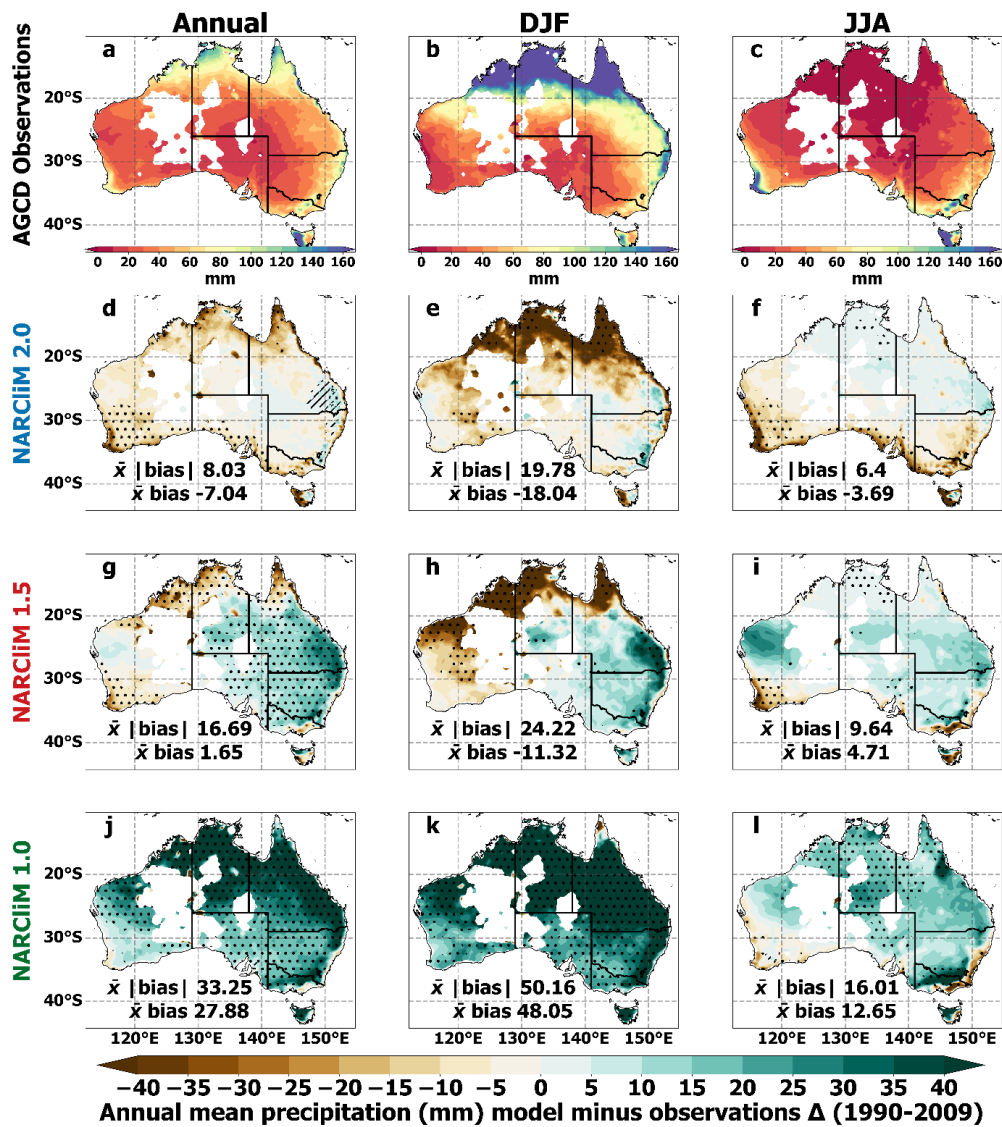
699 Figure 10. As per Figure 9 but for mean minimum temperature.

### 700 6.3 Precipitation

701 The NARClIM2.0 ensemble shows small dry biases for mean precipitation over most regions, except  
 702 for some areas mainly in the east of the country which show slight wet biases (Figure 11d-f). This  
 703 contrasts with stronger wet biases of NARClIM1.5 that are statistically significant over many regions  
 704 (Figure 11g-i) and the even stronger wet biases of NARClIM1.0 (Figure 11j-l). Area-averaged bias  
 705 magnitudes are considerably smaller for NARClIM2.0 relative to NARClIM1.x, especially for the annual  
 706 annual mean, i.e., 8.03 mm versus 16.69 mm and 33.25 mm, respectively. Annual mean precipitation

707 biases are particularly small over eastern regions, often being <5 mm. NARClIM2.0 retains the strong  
708 summertime dry biases for precipitation over northern Australia that are also evident for NARClIM1.5  
709 (Figure 11e,h), noting that this region also shows strong warm biases for maximum temperature (Fig-  
710 ure 9).

711         The individual RCMs comprising NARClIM2.0 show a range of results for annual and sea-  
712 sonal mean precipitation biases (Fig S12-S14). Notably, three of the ten NARClIM2.0 RCMs have  
713 substantially larger bias magnitudes than their peers at annual and summer timescales, i.e., both MPI-  
714 ESM1-2-HR-R3 and R5 (absolute biases are 15.53 mm and 22.45 mm for annual mean precipitation,  
715 Figure S12g-h) and EC-Earth3-Veg-R5 (Figure S12f; 18.59 mm). Despite EC-Earth3-Veg-R5 being  
716 strongly dry-biased, EC-Earth3-Veg-R3 simulates precipitation more accurately i.e., its mean absolute  
717 bias=9.53 mm (Figure S12e). Analogously to NARClIM2.0's performance for temperature, R5 is  
718 drier than R3. Comparing the ensemble means of the driving GCMs, the CMIP6 GCMs are margin-  
719 ally more accurate in simulating annual mean precipitation than the CMIP5 GCMs (Figure S15).  
720 Whilst the CMIP6 ensemble produces small biases over inland areas, its biases are larger along the  
721 east coast.

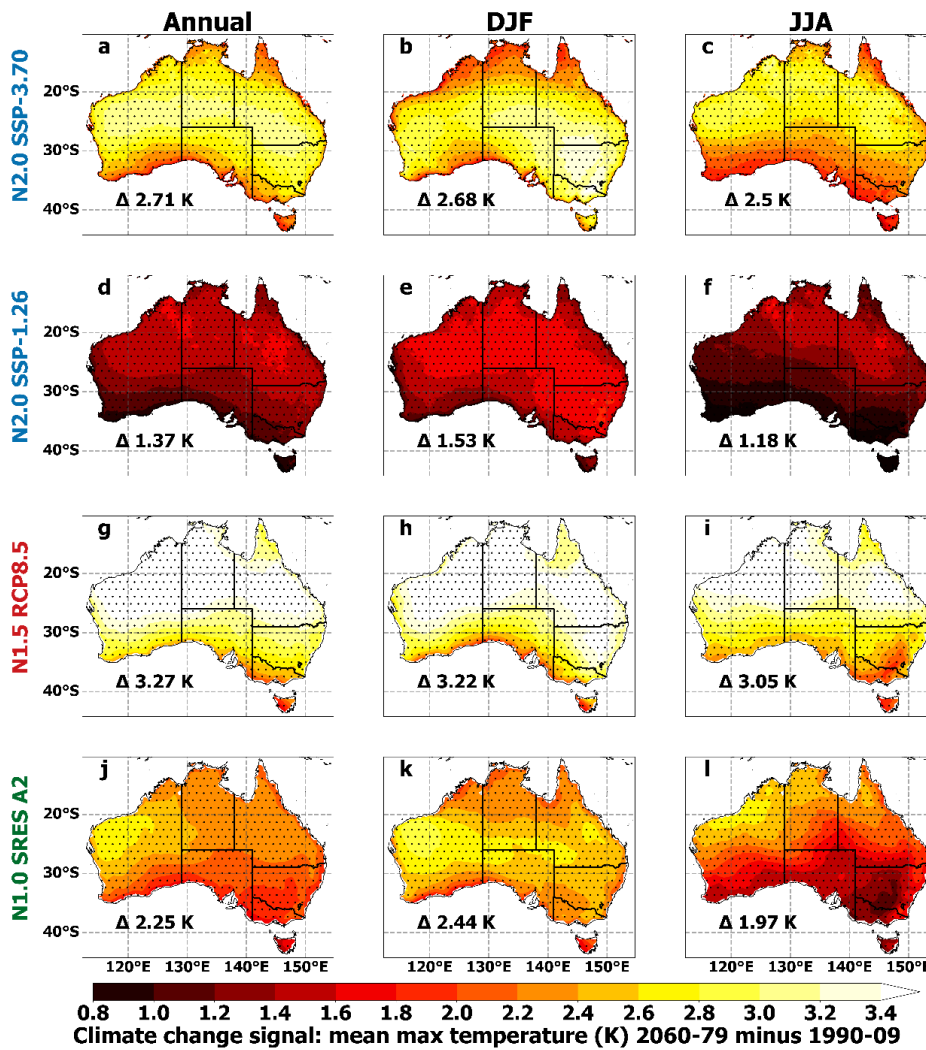


722  
723 **Figure 11.** As per Figure 9 but for mean precipitation (precip.).

## 724 **7. CORDEX-CMIP6 NARCIIM2.0 climate change projections**

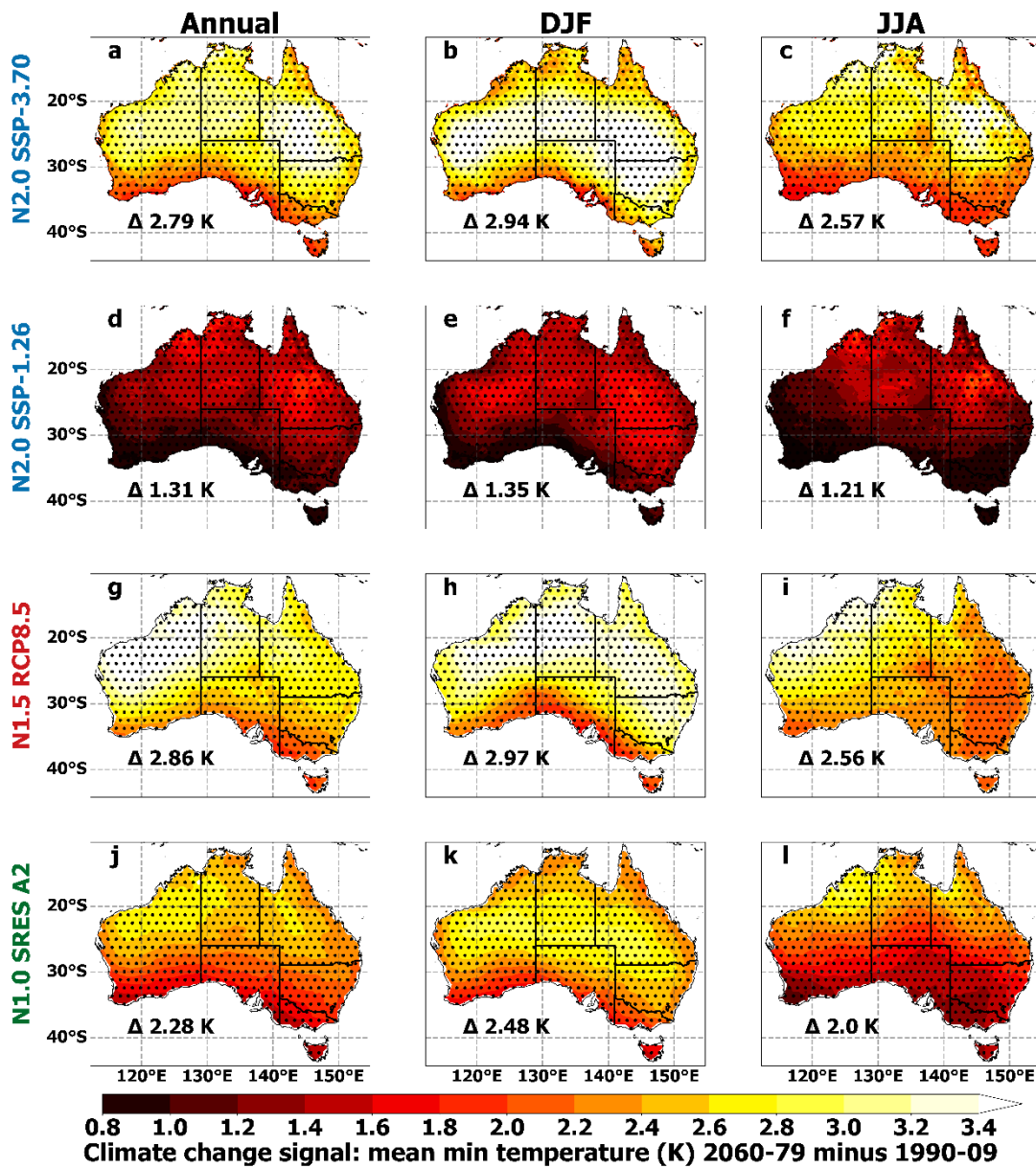
725 Dependent on location, the largest maximum temperature projected increases for NARCIIM2.0 under  
 726 SSP3-7.0 are over ~3 K, and over ~1.5 K under SSP1-2.6 (Figure 12a,d). SSP3-7.0-NARCIIM2.0  
 727 shows faster warming over inland than coastal regions, with greater warming across a horizontal band  
 728 of the continent during annual and summer timescales (Figure 12a-b). This contrasts with NAR-  
 729 CliM1.5 which shows a north-south warming gradient at annual and seasonal timescales, with its fast-  
 730 est warming rate over northern regions, and NARCIIM1.0 which projects fastest warming over the  
 731 west (Figure 12). For NARCIIM2.0, the tropical north warms faster during the winter dry season than  
 732 during the summer wet season under SSP3-7.0, but this is not the case for SSP1-2.6 (Figure 12b-c; e-  
 733 f). NARCIIM2.0 simulations under SSP3-7.0 show less warming than NARCIIM1.5-RCP8.5, but  
 734 warmer futures than for NARCIIM1.0-SRES A2, with differences in the underlying driving GCMs  
 735 and GHG scenarios likely contributing to these variations in warming. As per NARCIIM1.x, all

736 NARClIM2.0 maximum temperature projections are significant-agreeing with all RCMs projecting  
 737 statistically significant temperature increases.



738  
 739 **Figure 12.** Ensemble mean climate change projections (far future minus present-day) for annual, DJF and JJA  
 740 mean maximum temperatures with significance stippling as per Figure 9.

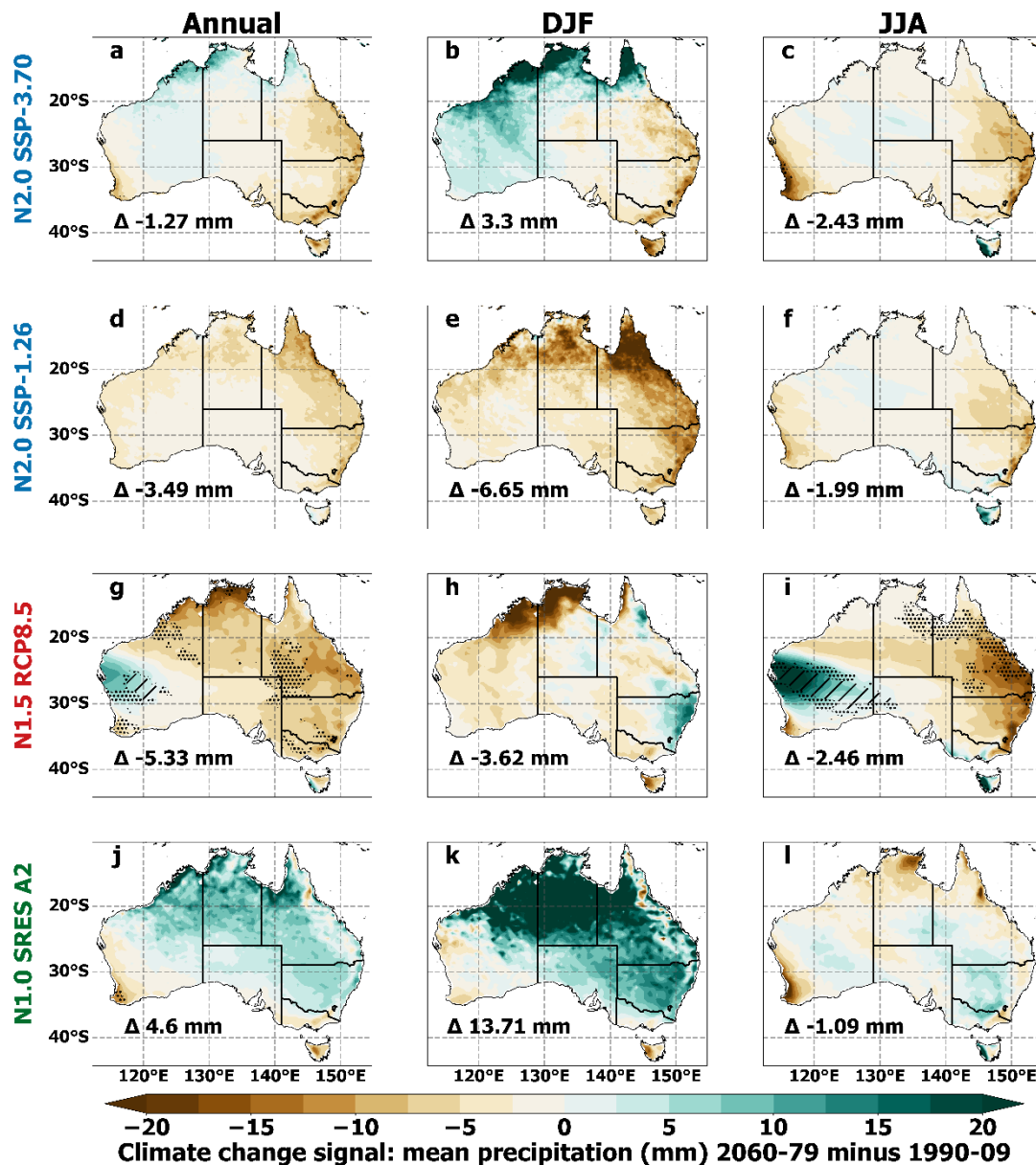
741 Projected increases in annual mean minimum temperature for NARClIM2.0 exceed 3 K over  
 742 some regions for SSP3-7.0, and 1.6 K for SSP1-2.6 (Figure 13). Under both GHG scenarios, at annual  
 743 and winter timescales warming is fastest over north-east Australia. Conversely, NARClIM1.x mini-  
 744 mum temperature future increases are generally largest over northwest or northern Australia, though  
 745 the summertime projection for NARClIM1.0 is an exception (Figure 13k). As for maximum tempera-  
 746 ture projections, all RCMs for all NARClIM generations project statistically significant increases.



747

748 **Figure 13.** Ensemble mean climate change projections (far future minus present-day) for annual, DJF and JJA  
 749 mean minimum temperatures with significance stippling as per Figure 9.

750 NARcliM2.0 SSP3-7.0 projects a dry future over most of Australia, except for wetter futures  
 751 over northern and western regions, which are largest in magnitude in summer (Figure 14a-b). In con-  
 752 trast, overall, NARcliM2.0 SSP1-2.6 projects dry changes across most of Australia, with the strongest  
 753 drying over northern Australia during summer (Figure 14e). Similarities between NARcliM2.0 pro-  
 754 jections for the low and high GHG SSPs include faster drying over the eastern coastline at all time-  
 755 scales, especially during summer. The wetter futures projected by RCMs downscaling SSP3-7.0-  
 756 GCMs relative to SSP1-2.6 may be partially inherited from the driving CMIP6 GCMs, because over-  
 757 all, SSP3-7.0 GCMs show wetter futures than corresponding SSP1-2.6 GCMs (Fig. S16).

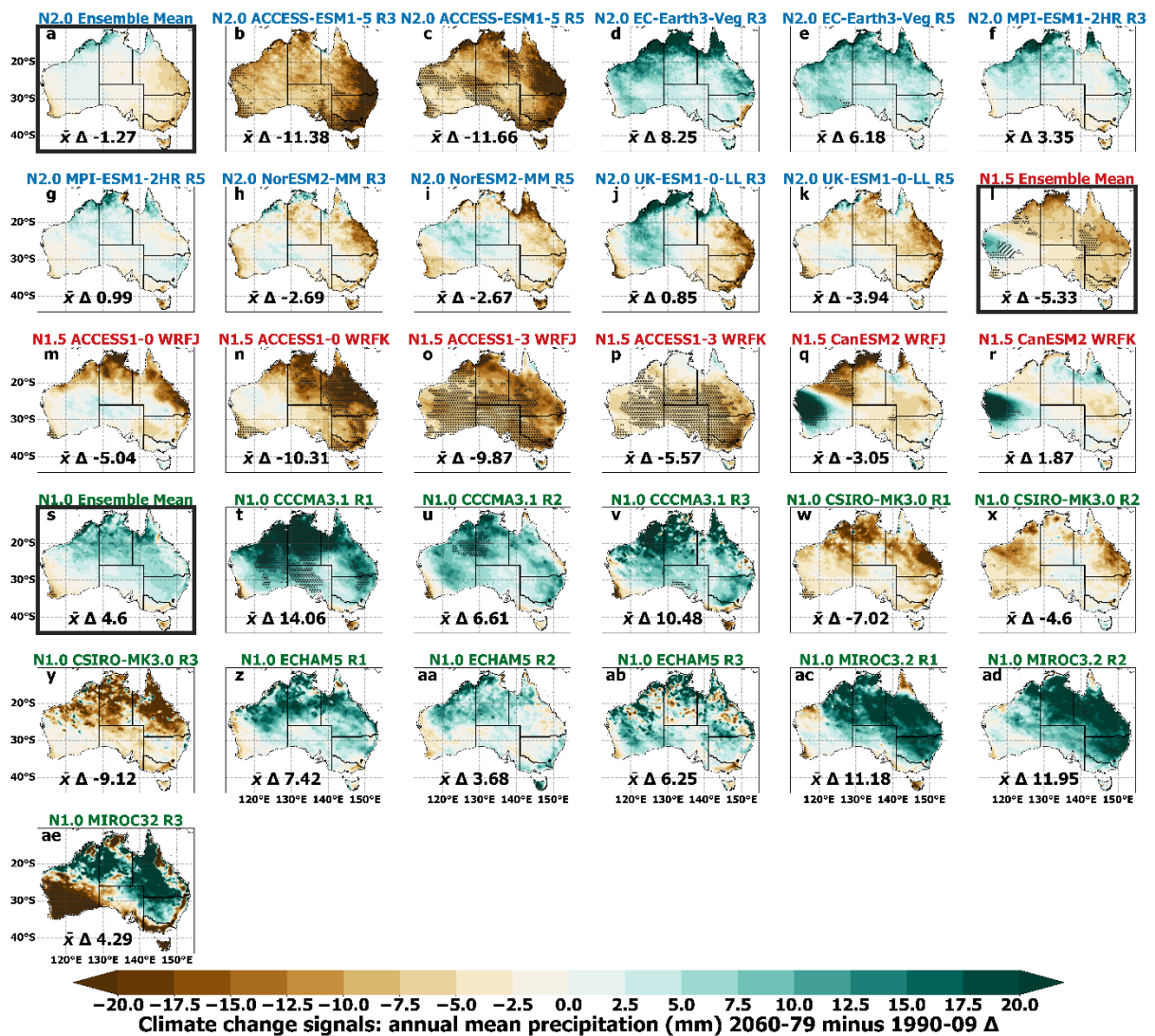


758

759 **Figure 14.** Ensemble mean climate change projections (far future minus present-day) for annual, DJF and JJA  
 760 mean precipitation with significance stippling as per Figure 9.

761 Considering mean precipitation projections for individual NARcliM2.0 RCMs, in some cases,  
 762 R3 and R5 RCMs produce similar results when downscaling the same GCM. For instance, ACCESS-  
 763 ESM-1-5 forced R3 and R5 both show strong projected decreases in annual mean precipitation across  
 764 Australia (Figure 15b-c). In contrast, while UK-ESM1-0-LL R3-R5 both show projected decreases in  
 765 annual mean precipitation over eastern Australia, R3 shows precipitation increases that are substan-  
 766 tially more widespread over western and northern regions relative to R5 (Figure 15j-k). Overall, the  
 767 NARcliM2.0 ensemble members show a variety of climate change signals for precipitation (Figure  
 768 15) and temperature (not shown), reflecting the range within the larger CMIP6 ensemble (Di Virgilio  
 769 et al. 2022).

770 There are some key differences between the mean precipitation projections of NARcliM2.0 rela-  
 771 tive to those of previous NARcliM generations. For instance, NARcliM1.5 shows stronger reduc-  
 772 tions in future precipitation over northern and eastern regions at annual and winter timescales (Figure  
 773 14), and these changes are statistically significant over a few regions, whereas projected changes for  
 774 NARcliM2.0 are largely non-significant. Additionally, NARcliM2.0 projects marked precipitation  
 775 decreases along the south-east coast during summer, while NARcliM1.5 shows the opposite result  
 776 (Figure 14). NARcliM1.0 generally projects wet futures across larger portions of Australia, especially  
 777 at annual and summer timescales.



779 **Figure 15.** Climate change projections (1990-2009 versus 2060-2079) for annual mean precipitation for NAR-  
 780 cliM ensemble mean climate change signals (a,l,s) and for individual ensemble members for each generation of  
 781 NARcliM simulation (NARcliM2.0 under SSP3-7.0, NARcliM1.5 under RCP8.5 and NARcliM1.0 under  
 782 SRES A2). Significance stippling as per Figure 9.

## 783 **8. Discussion and Summary**

784 NARClIM regional climate models produce robust climate projections at spatial scales suitable for  
785 local-scale climate change analysis and impact decision-making. The third and latest generation of  
786 these regional climate models, NARClIM2.0, encompasses several model design advancements over  
787 its predecessors. A key aim of this paper is to describe how NARClIM2.0 differs from its predeces-  
788 sors and explain the rationale for these design decisions. We also characterise the improvements in  
789 model skill in simulating the Australian climate relative to previous NARClIM generations, as well as  
790 compare climate projections across NARClIM generations. The next section discusses aspects of  
791 NARClIM2.0 RCM design and parameterisation in relation to previous studies before reviewing dif-  
792 ferences in the model biases and the climate projections of the NARClIM2.0 versus NARClIM 1.x  
793 RCMs.

### 794 **8.1 NARClIM2.0 RCM physics testing**

795 In addition to RCM design choices including increased resolution, and incorporation of convection-  
796 permitting modelling and urban physics, a major change for NARClIM2.0 relative to its predecessors  
797 is to use new WRF RCM configurations which are selected via a large suite of physics tests. RCM  
798 performance evaluations for the NARClIM2.0 RCM physics testing focused on the 4 km resolution  
799 convection-permitting domain which does not use a cumulus physics parameterisation. Notably, the 7  
800 candidate shortlisted RCMs from the N=78 physics test ensemble used three different cumulus param-  
801 eterisations for their outer domains, with 4 RCMs using BMJ, 2 RCMs using Tiedtke, and 1 using  
802 Kain-Fritsch. This indicates that differences in the outer domain boundary conditions have key influ-  
803 ences on the RCM performances in the convection-permitting domain.

804         Using the Noah-MP LSM in the NARClIM2.0 RCM physics tests conferred overall RCM  
805 skill improvements relative to RCMs using the Noah-Unified LSM, especially in terms of the simula-  
806 tion of temperature. Although using Noah-MP also improved the simulation of precipitation in some  
807 respects, these improvements were smaller relative to the gains for temperature, and improvements  
808 were mainly located over coastal regions. The developers of Noah-MP suggest that some limitations  
809 in the Noah-Unified LSM have been modified to better represent several parameters. These include  
810 surface layer radiation balances, snow depth, soil moisture and heat fluxes, leaf area-rainfall interac-  
811 tion, vegetation and canopy temperature distinction, drainage of soil, and runoff.

812         In the NARClIM2.0 physics testing, improvements in RCM skill were evident for Noah-MP  
813 with default settings. Activating specific parameterisations for this LSM (i.e. dynamic vegetation  
814 cover and surface runoff-simple groundwater) delivered comparatively smaller gains in RCM perfor-  
815 mances. Some previous studies have found no overall benefit of using Noah-MP with default settings.  
816 For instance, Imran et al. (2018) conducted an evaluation of WRF coupled with a variety of LSMs



817 including Noah-MP using its default settings. They simulated short-duration (~3-day) heatwaves in  
818 Melbourne, Australia and observed larger temperature biases using Noah-MP relative to RCMs using  
819 Noah-Unified and CLM4.0. However, their focus on specific short duration heatwave events over one  
820 urban area was not intended as a comprehensive evaluation of Noah-MP's performance. Additionally,  
821 several physics schemes used by these authors differed to those used in the NARClIM2.0 physics test-  
822 ing, i.e., they used: PBL=MYJ; microphysics=Thompson; cumulus=Grell3D; radia-  
823 tion=RRTMG/RRTMG. Only Thompson microphysics and RRTMG radiation are used in the NAR-  
824 ClIM2.0 physics testing. WRF and Noah-MP versions also differed, i.e., Imran et al. used WRF3.6.1  
825 and a Noah-MP version prior to 3.7, whereas NARClIM2.0 uses WRF4.1.2 and Noah-MP version 4.1.  
826 Additionally, there are also several studies that have reported benefits of using Noah-MP with default  
827 parameters relative to other LSMs for other regions globally e.g. Chen et al. (2014b), Chen et al.  
828 (2014a) and Salamanca et al. (2018).

829         The NARClIM2.0 physics testing found that the optimal LSM configuration for simulation of  
830 minimum temperature used Noah-MP with dynamic vegetation cover activated, even though the per-  
831 formance gain relative to Noah-MP with default settings was small. Constantinidou et al. (2020) ran  
832 WRF coupled with four LSMs (Noah-Unified, Noah-MP, CLM and, Rapid Update Cycle) over the  
833 Middle East North Africa CORDEX domain. They compared the performance of Noah-MP with dy-  
834 namic vegetation cover turned on and off and found that air and land temperatures were best simu-  
835 lated using Noah-MP with dynamic vegetation cover activated.

836         In terms of other NARClIM2.0 RCM parameterisations, focusing on PBL, by the completion  
837 of Phase I physics testing, only 3 of 12 RCMs shortlisted for further testing use the YSU scheme. By  
838 the completion of Phase II testing, all remaining RCMs using YSU are discarded, with only RCMs  
839 using PBL schemes other than YSU remaining (i.e., ACM2 and MYNN2). YSU PBL is a first-order  
840 closure scheme that expresses turbulent mixing via mean variables rather than prognostic variables  
841 (Hong et al., 2006). It is classed as a non-local scheme because it estimates turbulent mixing by small-  
842 scale eddies as well as representing transport caused by convective large eddies. Two previous studies  
843 evaluating convection permitting WRF simulations using different parameterisations that included  
844 YSU for the PBL scheme found that, relative to other PBL schemes, YSU produced the highest bias  
845 for simulated precipitation (Huang et al., 2023; Nuryanto et al., 2019). However, these studies focused  
846 on different regions globally and used various experimental setups that are not directly comparable to  
847 those used here. Hence, a separate study investigating sensitivities of the NARClIM2.0 RCMs to the  
848 different PBL schemes is currently underway.

## 849 **8.2 CORDEX-CMIP6 NARClIM2.0 historical evaluation**

850 We characterised the improvements conferred by NARClIM2.0 over its predecessors in simulating the  
851 present-day Australian climate. NARClIM2.0 simulates mean maximum temperature and precipitation

852 more accurately than NARClIM1.x. Specifically, NARClIM1.x has strong maximum temperature cold  
853 biases which are in keeping with other downscaling projects of the CMIP3-CMIP5 eras, e.g., (Andrys  
854 et al., 2016; Evans et al., 2020b), but these are substantially reduced in NARClIM2.0. A contributing  
855 cause of CMIP5-forced RCM cold biases of maximum temperature is their overestimation of precipi-  
856 tation (Evans et al., 2020). This relationship was also noted in ERA-Interim forced RCMs of this same  
857 modelling era (Di Virgilio et al. 2019). In NARClIM2.0, the widespread wet biases that characterise  
858 the NARClIM1.x RCMs are reduced in magnitude. NARClIM2.0 produces smaller wet biases over  
859 eastern Australia, and smaller dry biases elsewhere, except for Australia's tropical north. This marked  
860 reduction in wet bias magnitudes is one plausible contributing factor for the reduction in maximum  
861 temperature cold bias for the NARClIM2.0 RCMs. The CMIP6 and CMIP5 GCMs used to drive  
862 NARClIM2.0 and 1.5 RCMs generally show similar magnitudes of maximum temperature cold bias.  
863 This suggests that the underlying nature of the CMIP6 driving data is not a principal factor underlying  
864 the observed improvements for NARClIM2.0's simulation of maximum temperature. In fact, the  
865 RCMs appear to have a substantial influence on the reduced maximum temperature biases.

866 That NARClIM2.0 underestimates precipitation over tropical northern Australia during the  
867 wet season (summer) to a similar degree of magnitude to the NARClIM1.5 RCMs indicates that the  
868 newer models still struggle to accurately capture the strength of the Australian monsoon. That NAR-  
869 ClIM1.x strongly overestimates precipitation over south-eastern Australia whereas wet biases over  
870 this region are reduced for NARClIM2.0 indicates that the newer models may confer an improved  
871 simulation of broad-scale processes associated with synoptic-scale systems interacting with the extra-  
872 tropical storm track over Australia (Grose et al., 2019).

873 The extent to which NARClIM2.0's improved simulation of precipitation might be attributa-  
874 ble to its driving data warrants consideration. Overall, the CMIP6 GCMs used to drive NARClIM2.0  
875 show marginally reduced wet biases versus the CMIP5 GCMs used for NARClIM1.5 (e.g. area-aver-  
876 aged ensemble mean absolute biases are 7.13 mm and 8.89 mm, respectively; Supporting Information  
877 Figure S15). This suggests that the underlying nature of the CMIP6 driving data might not be the prin-  
878 cipal factor underlying the observed improvements for NARClIM2.0's simulation of mean precipita-  
879 tion. Conversely, in terms of RCM design features, the use of the Noah-MP LSM in the NARClIM2.0  
880 RCM physics tests conferred overall RCM skill improvements relative to RCMs using the Noah-Uni-  
881 fied LSM for both mean precipitation and mean maximum temperature. As noted above, the develop-  
882 ers of Noah-MP suggest that some features of the Noah-Unified LSM have been modified to better  
883 represent several parameters. The production NARClIM2.0 RCMs used Noah-MP, whereas NAR-  
884 ClIM1.x RCMs used Noah-Unified. Given these performance improvements observed for RCMs us-  
885 ing Noah-MP versus using Noah-Unified, it is plausible that the newer LSM contributes to the im-  
886 proved NARClIM2.0 skill in simulating precipitation and maximum temperature, for instance, via  
887 changing the land surface feedback (via soil moisture) to the simulation of precipitation. This possibil-  
888 ity requires more extensive investigation via future studies.

889 More generally, the scope of the present study was to focus on an initial "first-order" evalua-  
890 tion of mean precipitation rather than extremes of precipitation. However, clearly valuable research  
891 can now be undertaken into evaluating the skill of NARClIM2.0 in simulating extreme precipitation,  
892 subdaily precipitation, etc, using NARClIM2.0 20 km and 4 km data, noting these data are now pub-  
893 licly available. A good avenue for further research is to assess the potential added value in simulating  
894 extreme and subdaily precipitation at convection permitting scale versus the convection-parameterised  
895 20 km data. Several previous studies have confirmed that convection-permitting resolution models  
896 can improve the simulation of daily and sub-daily rainfall extremes (Xie et al., 2024; Cannon and  
897 Innocenti, 2019; Kendon et al., 2017).

898 NARClIM2.0 RCMs overestimate minimum temperatures across Australia, and these biases  
899 are larger relative to NARClIM1.5 but comparable to those of NARClIM1.0. The CMIP6 GCMs used  
900 to force NARClIM2.0 show substantially stronger warm biases for minimum temperature than the  
901 CMIP5 GCMs used for NARClIM1.5. This suggests that the increased warm bias for minimum tem-  
902 perature in NARClIM2.0-RCMs could be partially inherited from the driving GCMs. However,  
903 Noah-MP's simulation of factors such as LAI and other aspects of vegetation as well as surface al-  
904 bedo in semi-arid and arid areas has been shown to have deficiencies (Glotfelty et al., 2021). These  
905 issues may contribute to some of the biases shown by the NARClIM2.0 RCMs. Moreover, the NAR-  
906 ClIM2.0 ensemble mean reduces the overall minimum temperature bias of the CMIP6 GCM ensemble  
907 by almost half, attesting to the added value conferred by the NARClIM2.0 RCMs with respect to near-  
908 surface temperature variables.

909 Consideration of observational uncertainty is warranted. We have evaluated NARClIM RCM  
910 skill via comparison with AGCD observations. Whilst AGCD are a high quality gridded observational  
911 data set, like any set of observations, they contain errors and uncertainties. Consequently, the out-  
912 comes of our evaluations depend on both the models being evaluated and the AGCD observational  
913 dataset. This is clearly a broader issue that applies to any model evaluation versus observations. Un-  
914 certainties in AGCD for temperature and precipitation arise from sparse station coverage in some lo-  
915 cations, especially in remote areas, and interpolation errors in generating gridded data. More specifi-  
916 cally, temperature uncertainties include urban heat island effects, inhomogeneities in observation rec-  
917 ords, and elevation differences. Precipitation uncertainties involve underestimation of extremes, rain  
918 gauge measurement errors, and challenges in representing complex terrain. For our purposes, the  
919 question of how much of a model bias of  $\sim 0.5$  K is due to the model errors versus the observational  
920 uncertainty cannot be currently quantified, because the models are evaluated against this single obser-  
921 vational dataset. This leaves the observational uncertainty as implicitly included in our results. In the  
922 future observational uncertainty could be explicitly considered using a method like the Observation  
923 Range Adjusted (ORA) statistics (Evans and Imran, 2024).

### 924 **8.3 CORDEX-CMIP6 NARClIM2.0 climate change projections**

925 In terms of NARClIM2.0 future climate projections, major changes between NARClIM generations  
926 such as differences in GHG scenarios mean that NARClIM2.0 projected temperature changes differ in  
927 some respects to those of its predecessors. Overall, as is expected, projected warming is less intense in  
928 NARClIM2.0 under SSP3-7.0 than for NARClIM1.5 under RCP8.5. Other differences in the projec-  
929 tions between NARClIM generations require further investigation in order to explain, such as NAR-  
930 ClIM1.5's latitudinal warming gradient for maximum temperature that contrasts with NARClIM2.0's  
931 band of faster warming over central Australia relative to northern and southern regions. Irrespective of  
932 these differences, all three NARClIM ensembles show widespread statistically significant-agreeing  
933 results for warming projections.

934         Precipitation projections for the different NARClIM generations show some key similarities,  
935 such as reductions in mean annual precipitation over eastern Australia for NARClIM2.0 and NAR-  
936 ClIM1.5, though a difference is that these are statistically significant over some areas only for NAR-  
937 ClIM1.5. The NARClIM2.0-SSP3-7.0 and SSP1-2.6 ensembles differ in that the former generally pro-  
938 jects wet changes over northern and western Australia, whereas the latter is generally dry, results that  
939 appear partially traceable to the underlying driving CMIP6-SSP data (Supporting Information Figure  
940 S16).

941         Some NARClIM2.0 RCMs produce very similar precipitation projections for certain GCM-  
942 RCM combinations. Notably, ACCESS-ESM-1-5-R3 and R5 under SSP3-7.0 both produce wide-  
943 spread dry projections that are substantially drier than other NARClIM2.0 models. This GCM projects  
944 very dry futures across Australia (Di Virgilio et al., 2022), so this result in the R3 and R5 RCMs could  
945 be largely inherited from the driving data. There are 40 realisations for ACCESS-ESM1-5, but only  
946 realisation 6 provides sub-daily outputs that can be used in dynamical downscaling using WRF. This  
947 realisation simulates a particularly dry projection over Australia, especially for eastern Australia,  
948 making it a useful "stress test" case. In terms of GCM skill versus observations, globally, this GCM is  
949 dry biased over a few regions owing to a location bias with the Inter-tropical Convergence Zone  
950 (Rashid et al., 2022; Ziehn et al., 2020).

951         In other instances, there are marked divergences between the NARClIM2.0 R3 versus R5 pre-  
952 cipitation projections when forced with the same GCM. An example is UK-ESM-1-0-LL under SSP3-  
953 7.0 where R3 projects stronger precipitation increases that are more geographically widespread rela-  
954 tive to R5. This raises the question of varying sources of uncertainty in the climate projections, i.e., to  
955 what extent these are attributable to GCMs versus RCMs, as well as other factors.

## 956 **8.4 Summary**

957 In summary, the CORDEX-CMIP6 NARClIM2.0 regional climate projections are a 10-member en-  
958 semble comprising two configurations of the WRF RCM dynamically downscaling five GCMs under  
959 three SSPs at 20 km resolution over CORDEX-Australasia and at 4 km convection-permitting resolu-  
960 tion over south-east Australia. In addition to several high-level model design changes, e.g., increased  
961 spatial resolution, a large (N=78) RCM-physics test suite is evaluated to select two new WRF RCM  
962 configurations for CMIP6-forced NARClIM2.0 climate projections. The NARClIM2.0 physics tests  
963 identified RCM configurations that generally performed well in simulating the recent Australian cli-  
964 mate over southeast Australia. A key finding was that WRF RCMs using the Noah-MP LSM gener-  
965 ally out-performed RCMs using other LSMs in representing regional climate. Despite the overall per-  
966 formance gains evident for RCMs using Noah-MP, these improvements were superior over temper-  
967 ate/coastal regions of southeast Australia relative to the semi-arid interior. These performance charac-  
968 teristics might be linked to Noah-MP's development being focused on Northern Hemisphere mid-lati-  
969 tudes, including assumptions such as accounting for differences in seasonality in the Northern versus  
970 Southern Hemispheres by shifting the Northern Hemisphere LAI profiles by 6 months. For the south-  
971 east Australian context, noting its distinctive coastal dry-sclerophyll and expansive inland grassland  
972 biomes, such assumptions might lead to discontinuities in quantities such as LAI. Given the geo-  
973 graphic focus of Noah-MP's development, as well as its performance characteristics, it may be more  
974 suited to application over the temperate regions of Australia rather than the semi-arid interior. It is  
975 also possible that modifying/tuning Noah-MP to specific aspects of the Australian context would yield  
976 performance benefits for follow-up dynamical downscaling.

977 Overall, the CMIP6-NARClIM2.0 ensemble produces a good representation of recent mean  
978 climate that in several key respects improves upon the model skill of earlier NARClIM generations.  
979 This study provides a foundation for more detailed investigations of the model biases and future cli-  
980 mate changes described here, including process-focused studies exploring their mechanisms.  
981 CORDEX-CMIP6 NARClIM2.0 RCM data provide valuable resources to investigate projected cli-  
982 mate changes, their impacts on societies and natural systems, and potential climate change mitigation  
983 and adaptation actions for the CORDEX-Australasia region.

## 984 **9. Code Availability**

985 A frozen version of the source code for the Weather Research and Forecasting (WRF) version 4.1.2  
986 used in this study, as well as the configuration files for the simulations, is available on Zenodo at:  
987 <https://doi.org/10.5281/zenodo.11184830>

## 988 **10. Data Availability**

989 Data for the NARClIM2.0 CMIP6-forced R3 and R5 RCMs are being made available via [National](#)  
990 [Computing Infrastructure](#) (NCI). WRF namelist settings for the NARClIM2.0 CMIP6-forced R3 and  
991 R5 RCMs are shown in Supplementary Material Figure S1 and are also available at:  
992 <https://doi.org/10.5281/zenodo.11184830>. Data NARClIM1.5 RCMs are available via the [New South](#)  
993 [Wales Climate Data Portal](#) and [CORDEX-DKRZ](#). Data for NARClIM1.0 RCMs are available via the  
994 [New South Wales Climate Data Portal](#). CMIP6 GCM data are available via the [Earth System Grid](#)  
995 [Federation](#).

## 996 **11. Author Contribution**

997 GDV and JPE designed the models and the simulations. FJ, ET, JA, and CT setup the models and  
998 conducted the model simulations with contributions from JPE, JK, DC, CR, SW, YL, MER, RG and  
999 JL. GDV prepared the manuscript with contributions from all co-authors.

## 1000 **12. Competing Interests**

1001 The authors declare that they have no conflict of interest, noting that JK has been a Topic Editor of  
1002 Geoscientific Model Development from 2015 to 2024.

## 1003 **13. Funding**

1004 This research was supported by the New South Wales Department of Climate Change, Energy, the  
1005 Environment and Water as part of the NARClIM2.0 dynamical downscaling project contributing to  
1006 CORDEX Australasia. Funding was provided by the NSW Climate Change Fund, the NSW Climate  
1007 Change Adaptation Strategy Program, and the ACT, SA, WA and VIC Governments for the NSW and  
1008 Australia Regional Climate Modelling (NARClIM) Project. This research was undertaken with the  
1009 assistance of resources and services from the National Computational Infrastructure (NCI), which is  
1010 supported by the Australian Government.

1011 Jason P. Evans acknowledges the support of the Australian Research Council Centre of Excellence for  
1012 Climate Extremes (CE170100023) and the Climate Systems Hub of the Australian Governments  
1013 National Environmental Science Program.

## 1014 **14. Acknowledgements**

1015 All authors thank the reviewers for their thoughtful and insightful feedback on this manuscript, and  
1016 the Editor at Geoscientific Model Development for handling the peer review process of this  
1017 manuscript.

## 1018 **15. References**

- 1019 Andrys, J., Lyons, T. J., and Kala, J.: Evaluation of a WRF ensemble using GCM boundary conditions  
1020 to quantify mean and extreme climate for the southwest of Western Australia (1970–1999),  
1021 International Journal of Climatology, 36, 4406–4424, <https://doi.org/10.1002/joc.4641>, 2016.
- 1022 Australian Bureau of Statistics.: Regional population, Online at:  
1023 <https://www.abs.gov.au/statistics/people/population/regional-population/latest-release>, 2024.
- 1024 Bjordal, J., Storelvmo, T., Alterskjaer, K., and Carlsen, T.: Equilibrium climate sensitivity above 5  
1025 degrees C plausible due to state-dependent cloud feedback, Nat. Geosci., 13, 718–+,  
1026 10.1038/s41561-020-00649-1, 2020.
- 1027 Bureau of Meteorology.: Annual climate statement 2016, 2017.
- 1028 Cannon, A. J. and Innocenti, S.: Projected intensification of sub-daily and daily rainfall extremes in  
1029 convection-permitting climate model simulations over North America: implications for future  
1030 intensity–duration–frequency curves, Nat. Hazards Earth Syst. Sci., 19, 421–440,  
1031 10.5194/nhess-19-421-2019, 2019.
- 1032 Chen, F., Liu, C. H., Dudhia, J., and Chen, M.: A sensitivity study of high-resolution regional climate  
1033 simulations to three land surface models over the western United States, Journal of  
1034 Geophysical Research-Atmospheres, 119, 7271–7291, 10.1002/2014jd021827, 2014a.
- 1035 Chen, F., Barlage, M., Tewari, M., Rasmussen, R., Jin, J. M., Lettenmaier, D., Livneh, B., Lin, C. Y.,  
1036 Miguez-Macho, G., Niu, G. Y., Wen, L. J., and Yang, Z. L.: Modeling seasonal snowpack  
1037 evolution in the complex terrain and forested Colorado Headwaters region: A model  
1038 intercomparison study, Journal of Geophysical Research-Atmospheres, 119, 13795–13819,  
1039 10.1002/2014jd022167, 2014b.
- 1040 Chou, M. D., Suarez, M. J., Liang, X. Z., and Yan, M. M. H.: A thermal infrared radiation  
1041 parameterization for atmospheric studies, NASA Tech. Memo. NASA/TM-2001-104606, 19,  
1042 68 pp. <https://ntrs.nasa.gov/citations/20010072848>, 2001.
- 1043 Constantinidou, K., Hadjinicolaou, P., Zittis, G., and Lelieveld, J.: Performance of Land Surface  
1044 Schemes in the WRF Model for Climate Simulations over the MENA-CORDEX Domain,  
1045 Earth Systems and Environment, 19, 10.1007/s41748-020-00187-1, 2020.
- 1046 Dee, D. P., Uppala, S. M., Simmons, A. J., Berrisford, P., Poli, P., Kobayashi, S., Andrae, U.,  
1047 Balmaseda, M. A., Balsamo, G., Bauer, P., Bechtold, P., Beljaars, A. C. M., van de Berg, L.,

1048 Bidlot, J., Bormann, N., Delsol, C., Dragani, R., Fuentes, M., Geer, A. J., Haimberger, L.,  
1049 Healy, S. B., Hersbach, H., Hólm, E. V., Isaksen, L., Kållberg, P., Köhler, M., Matricardi, M.,  
1050 McNally, A. P., Monge-Sanz, B. M., Morcrette, J. J., Park, B. K., Peubey, C., de Rosnay, P.,  
1051 Tavolato, C., Thépaut, J. N., and Vitart, F.: The ERA-Interim reanalysis: configuration and  
1052 performance of the data assimilation system, *Quarterly Journal of the Royal Meteorological*  
1053 *Society*, 137, 553-597, 10.1002/qj.828, 2011.

1054 Di Virgilio, G., Evans, J. P., Di Luca, A., Olson, R., Argüeso, D., Kala, J., Andrys, J., Hoffmann, P.,  
1055 Katzfey, J. J., and Rockel, B.: Evaluating reanalysis-driven CORDEX regional climate  
1056 models over Australia: model performance and errors, *Clim. Dyn.*, 53, 2985-3005,  
1057 10.1007/s00382-019-04672-w, 2019.

1058 Di Virgilio, G., Ji, F., Tam, E., Nishant, N., Evans, J. P., Thomas, C., Riley, M. L., Beyer, K., Grose,  
1059 M. R., Narsey, S., and Delage, F.: Selecting CMIP6 GCMs for CORDEX Dynamical  
1060 Downscaling: Model Performance, Independence, and Climate Change Signals, *Earth's*  
1061 *Future*, 10, e2021EF002625, <https://doi.org/10.1029/2021EF002625>, 2022.

1062 Di Virgilio, G., Ji, F., Tam, E., Evans, J. P., Kala, J., Andrys, J., Thomas, C., Choudhury, D., Rocha,  
1063 C., Li, Y., Riley, M.: Evaluation of CORDEX ERA5-forced 'NARClIM2. 0' regional climate  
1064 models over Australia using the Weather Research and Forecasting (WRF) model version  
1065 4.1.2, *Geoscientific Model Development*, <https://doi.org/10.5194/gmd-2024-41>, 2024.

1066 DWER.: *Climate Adaptation Strategy - Building WA's Climate Resilient Future*, Government of  
1067 Western Australia, 25 pages. Online at: [https://www.wa.gov.au/system/files/2023-](https://www.wa.gov.au/system/files/2023-07/climate_adaption_strategy_220623.pdf)  
1068 [07/climate\\_adaption\\_strategy\\_220623.pdf](https://www.wa.gov.au/system/files/2023-07/climate_adaption_strategy_220623.pdf), 2023.

1069 Evans, A., Jones, D., Lellyett, S., and Smalley, R.: An Enhanced Gridded Rainfall Analysis Scheme  
1070 for Australia, Australian Bureau of Meteorology 2020a.

1071 Evans, J. P. and Imran, H. M.: The observation range adjusted method: a novel approach to  
1072 accounting for observation uncertainty in model evaluation, *Environmental Research*  
1073 *Communications*, 6, 071001, 10.1088/2515-7620/ad5ad8, 2024.

1074 Evans, J. P., Ji, F., Lee, C., Smith, P., Argüeso, D., and Fita, L.: Design of a regional climate  
1075 modelling projection ensemble experiment - NARClIM, *Geosci. Model Dev.*, 7, 621-629,  
1076 10.5194/gmd-7-621-2014, 2014.

1077 Evans, J. P., Di Virgilio, G., Hirsch, A. L., Hoffmann, P., Remedio, A. R., Ji, F., Rockel, B., and  
1078 Coppola, E.: The CORDEX-Australasia ensemble: evaluation and future projections, *Clim.*  
1079 *Dyn.*, 10.1007/s00382-020-05459-0, 2020b.

1080 Fiddes, S., Pepler, A., Saunders, K., and Hope, P.: Redefining southern Australia's climatic regions  
1081 and seasons, *J. South Hemisph. Earth Syst. Sci.*, 71, 92-109, <https://doi.org/10.1071/ES20003>,  
1082 2021.



1083 Giorgi, F.: Thirty Years of Regional Climate Modeling: Where Are We and Where Are We Going  
1084 next?, *Journal of Geophysical Research: Atmospheres*, 124, 5696-5723,  
1085 10.1029/2018jd030094, 2019.

1086 Glotfelty, T., Ramírez-Mejía, D., Bowden, J., Ghilardi, A., and West, J. J.: Limitations of WRF land  
1087 surface models for simulating land use and land cover change in Sub-Saharan Africa and  
1088 development of an improved model (CLM-AF v. 1.0), *Geosci. Model Dev.*, 14, 3215-3249,  
1089 10.5194/gmd-14-3215-2021, 2021.

1090 Grose, M., Narsey, S., Trancoso, R., Mackallah, C., Delage, F., Dowdy, A., Di Virgilio, G.,  
1091 Watterson, I., Dobrohotoff, P., Rashid, H. A., Rauniyar, S., Henley, B., Thatcher, M., Syktus,  
1092 J., Abramowitz, G., Evans, J. P., Su, C.-H., and Takbash, A.: A CMIP6-based multi-model  
1093 downscaling ensemble to underpin climate change services in Australia, *Climate Services*, 30,  
1094 100368, <https://doi.org/10.1016/j.cliser.2023.100368>, 2023.

1095 Grose, M. R., Foster, S., Risbey, J. S., Osbrough, S., and Wilson, L.: Using indices of atmospheric  
1096 circulation to refine southern Australian winter rainfall climate projections, *Clim. Dyn.*,  
1097 10.1007/s00382-019-04880-4, 2019.

1098 Grose, M. R., Narsey, S., Delage, F., Dowdy, A. J., Bador, M., Boschhat, G., Chung, C., Kajtar, J.,  
1099 Rauniyar, S., Freund, M., Lyu, K., Rashid, H. A., Zhang, X., Wales, S., Trenham, C.,  
1100 Holbrook, N. J., Cowan, T., Alexander, L. V., Arblaster, J. M., and Power, S. B.: Insights  
1101 from CMIP6 for Australia's future climate, *Earth's Future*, 8, e2019EF001469,  
1102 <https://doi.org/10.1029/2019EF001469>, 2020.

1103 Herger, N., Abramowitz, G., Knutti, R., Angéilil, O., Lehmann, K., and Sanderson, B. M.: Selecting a  
1104 climate model subset to optimise key ensemble properties, *Earth Syst. Dynam.*, 9, 135-151,  
1105 10.5194/esd-9-135-2018, 2018.

1106 Hong, S.-Y., Noh, Y., and Dudhia, J.: A New Vertical Diffusion Package with an Explicit Treatment  
1107 of Entrainment Processes, *Monthly Weather Review*, 134, 2318-2341,  
1108 <https://doi.org/10.1175/MWR3199.1>, 2006.

1109 Hong, S. Y. and Lim, J.-O. J.: The WRF Single-Moment 6-Class Microphysics Scheme (WSM6),  
1110 *Asia-Pac. J. Atmos. Sci.*, 42, 129-151, 2006.

1111 Hsiang, S., Kopp, R., Jina, A., Rising, J., Delgado, M., Mohan, S., Rasmussen, D. J., Muir-Wood, R.,  
1112 Wilson, P., Oppenheimer, M., Larsen, K., and Houser, T.: Estimating economic damage from  
1113 climate change in the United States, *Science*, 356, 1362-1368, 10.1126/science.aal4369, 2017.

1114 Huang, Y., Xue, M., Hu, X.-M., Martin, E., Novoa, H. M., McPherson, R. A., Perez, A., and Morales,  
1115 I. Y.: Convection-Permitting Simulations of Precipitation over the Peruvian Central Andes:  
1116 Strong Sensitivity to Planetary Boundary Layer Parameterization, *J. Hydrometeorol.*, 24,  
1117 1969-1990, <https://doi.org/10.1175/JHM-D-22-0173.1>, 2023.

1118 Iacono, M. J., Delamere, J. S., Mlawer, E. J., Shephard, M. W., Clough, S. A., and Collins, W. D.:  
1119 Radiative forcing by long-lived greenhouse gases: Calculations with the AER radiative

1120 transfer models, *Journal of Geophysical Research: Atmospheres*, 113,  
1121 <https://doi.org/10.1029/2008JD009944>, 2008.

1122 Imran, H. M., Kala, J., Ng, A. W. M., and Muthukumar, S.: An evaluation of the performance of a  
1123 WRF multi-physics ensemble for heatwave events over the city of Melbourne in southeast  
1124 Australia, *Clim. Dyn.*, 50, 2553-2586, 10.1007/s00382-017-3758-y, 2018.

1125 IPCC: *Climate Change 2021: The Physical Science Basis. Contribution of Working Group I to the*  
1126 *Sixth Assessment Report of the Intergovernmental Panel on Climate Change*, Cambridge  
1127 University Press, 2021.

1128 Iturbide, M., Gutiérrez, J. M., Alves, L. M., Bedia, J., Cerezo-Mota, R., Gimpeanu, E., Cofiño, A.  
1129 S., Di Luca, A., Faria, S. H., Gorodetskaya, I. V., Hauser, M., Herrera, S., Hennessy, K.,  
1130 Hewitt, H. T., Jones, R. G., Krakovska, S., Manzanar, R., Martínez-Castro, D., Narisma, G.  
1131 T., Nurhati, I. S., Pinto, I., Seneviratne, S. I., van den Hurk, B., and Vera, C. S.: An update of  
1132 IPCC climate reference regions for subcontinental analysis of climate model data: definition  
1133 and aggregated datasets, *Earth Syst. Sci. Data*, 12, 2959-2970, 10.5194/essd-12-2959-2020,  
1134 2020.

1135 Janjić, Z. I.: Comments on “Development and Evaluation of a Convection Scheme for Use in Climate  
1136 Models”, *Journal of the Atmospheric Sciences*, 57, 3686-3686, [https://doi.org/10.1175/1520-0469\(2000\)057<3686:CODAEO>2.0.CO;2](https://doi.org/10.1175/1520-0469(2000)057<3686:CODAEO>2.0.CO;2), 2000.

1137  
1138 Kain, J. S.: The Kain-Fritsch convective parameterization: An update, *Journal of Applied*  
1139 *Meteorology*, 43, 170-181, 10.1175/1520-0450(2004)043<0170:tkcpau>2.0.co;2, 2004.

1140 Kendon, E. J., Prein, A. F., Senior, C. A., and Stirling, A.: Challenges and outlook for convection-  
1141 permitting climate modelling, *Philosophical transactions. Series A, Mathematical, physical,*  
1142 *and engineering sciences*, 379, 20190547, 10.1098/rsta.2019.0547, 2021.

1143 Kendon, E. J., Ban, N., Roberts, N. M., Fowler, H. J., Roberts, M. J., Chan, S. C., Evans, J. P., Fosse, G.,  
1144 and Wilkinson, J. M.: Do convection-permitting regional climate models improve  
1145 projections of future precipitation change?, *Bulletin of the American Meteorological Society*,  
1146 98, 79-+, 10.1175/bams-d-15-0004.1, 2017.

1147 King, A. D., Alexander, L. V., and Donat, M. G.: The efficacy of using gridded data to examine  
1148 extreme rainfall characteristics: a case study for Australia, *International Journal of*  
1149 *Climatology*, 33, 2376-2387, 10.1002/joc.3588, 2013.

1150 Kusaka, H. and Kimura, F.: Coupling a Single-Layer Urban Canopy Model with a Simple  
1151 Atmospheric Model: Impact on Urban Heat Island Simulation for an Idealized Case, *Journal*  
1152 *of the Meteorological Society of Japan. Ser. II*, 82, 67-80, 10.2151/jmsj.82.67, 2004.

1153 Lee, D., Min, S.-K., Ahn, J.-B., Cha, D.-H., Shin, S.-W., Chang, E.-C., Suh, M.-S., Byun, Y.-H., and  
1154 Kim, J.-U.: Uncertainty analysis of future summer monsoon duration and area over East Asia  
1155 using a multi-GCM/multi-RCM ensemble, *Environ. Res. Lett.*, 18, 064026, 10.1088/1748-  
1156 9326/acd208, 2023.

1157 Lucas-Picher, P., Argüeso, D., Brisson, E., Trambly, Y., Berg, P., Lemonsu, A., Kotlarski, S., and  
1158 Caillaud, C.: Convection-permitting modeling with regional climate models: Latest  
1159 developments and next steps, *WIREs Climate Change*, 12, e731,  
1160 <https://doi.org/10.1002/wcc.731>, 2021.

1161 Meehl, G. A., Senior, C. A., Eyring, V., Flato, G., Lamarque, J.-F., Stouffer, R. J., Taylor, K. E., and  
1162 Schlund, M.: Context for interpreting equilibrium climate sensitivity and transient climate  
1163 response from the CMIP6 Earth system models, *Science Advances*, 6, eaba1981,  
1164 10.1126/sciadv.aba1981, 2020.

1165 Murphy, B. F. and Timbal, B.: A review of recent climate variability and climate change in  
1166 southeastern Australia, *International Journal of Climatology*, 28, 859-879,  
1167 <https://doi.org/10.1002/joc.1627>, 2008.

1168 Nakanishi, M. and Niino, H.: Development of an Improved Turbulence Closure Model for the  
1169 Atmospheric Boundary Layer, *Journal of the Meteorological Society of Japan. Ser. II*, 87,  
1170 895-912, 10.2151/jmsj.87.895, 2009.

1171 Nishant, N., Evans, J. P., Di Virgilio, G., Downes, S. M., Ji, F., Cheung, K. K. W., Tam, E., Miller, J.,  
1172 Beyer, K., and Riley, M. L.: Introducing NARClM1.5: Evaluating the Performance of  
1173 Regional Climate Projections for Southeast Australia for 1950–2100, *Earth's Future*, 9,  
1174 e2020EF001833, <https://doi.org/10.1029/2020EF001833>, 2021.

1175 Niu, G.-Y., Yang, Z.-L., Mitchell, K. E., Chen, F., Ek, M. B., Barlage, M., Kumar, A., Manning, K.,  
1176 Niyogi, D., Rosero, E., Tewari, M., and Xia, Y.: The community Noah land surface model  
1177 with multiparameterization options (Noah-MP): 1. Model description and evaluation with  
1178 local-scale measurements, *Journal of Geophysical Research: Atmospheres*, 116,  
1179 10.1029/2010jd015139, 2011.

1180 NSW Government.: NSW Climate Change Fund Annual Report 2021-22, 2022.

1181 NSW Government.: NSW Climate Change Fund Annual Report 2022-23, 2023.

1182 Nuryanto, D. E., Satyaningsih, R., Nuraini, T. A., Rizal, J., Heriyanto, E., Linarka, U. A., and  
1183 Sopaheluwakan, A.: Evaluation of Planetary Boundary Layer (PBL) schemes in simulating  
1184 heavy rainfall events over Central Java using high resolution WRF model, *Sixth International  
1185 Symposium on LAPAN-IPB Satellite, SPIE*, 2019.

1186 Oleson, K., Lawrence, D., Bonan, G. B., Flanner, M., Kluzek, E., Lawrence, P., Levis, S., Swenson,  
1187 S. C., Thornton, P. E., Dai, A., Decker, M., Dickinson, R., Feddema, J., Heald, C., Hoffman,  
1188 F., Lamarque, J.-F., Mahowald, N., Niu, G.-Y., Qian, T., and Zeng, X.: Technical Description  
1189 of version 4.0 of the Community Land Model (CLM), 2010.

1190 Pepler, A. and Dowdy, A.: Intense east coast lows and associated rainfall in eastern Australia, *J. South  
1191 Hemisph. Earth Syst. Sci.*, 71, 110-122, 10.1071/es20013, 2021.

1192 Perkins, S. E., Pitman, A. J., Holbrook, N. J., and McAneney, J.: Evaluation of the AR4 climate  
1193 models' simulated daily maximum temperature, minimum temperature, and precipitation over

1194 Australia using probability density functions, *J. Clim.*, 20, 4356-4376, 10.1175/jcli4253.1,  
1195 2007.

1196 Pleim, J. E.: A Combined Local and Nonlocal Closure Model for the Atmospheric Boundary Layer.  
1197 Part I: Model Description and Testing, *J. Appl. Meteorol. Climatol.*, 46, 1383-1395,  
1198 <https://doi.org/10.1175/JAM2539.1>, 2007.

1199 Rashid, H. A., Sullivan, A., Dix, M., Bi, D., Mackallah, C., Ziehn, T., Dobrohotoff, P., O'Farrell, S.,  
1200 Harman, I. N., Bodman, R., and Marsland, S.: Evaluation of climate variability and change in  
1201 ACCESS historical simulations for CMIP6, *J. South Hemisph. Earth Syst. Sci.*, 72, 73-92,  
1202 <https://doi.org/10.1071/ES21028>, 2022.

1203 Salamanca, F., Zhang, Y. Z., Barlage, M., Chen, F., Mahalov, A., and Miao, S. G.: Evaluation of the  
1204 WRF-Urban Modeling System Coupled to Noah and Noah-MP Land Surface Models Over a  
1205 Semiarid Urban Environment, *Journal of Geophysical Research-Atmospheres*, 123, 2387-  
1206 2408, 10.1002/2018jd028377, 2018.

1207 Sherwood, S. C., Webb, M. J., Annan, J. D., Armour, K. C., Forster, P. M., Hargreaves, J. C., Hegerl,  
1208 G., Klein, S. A., Marvel, K. D., Rohling, E. J., Watanabe, M., Andrews, T., Braconnot, P.,  
1209 Bretherton, C. S., Foster, G. L., Hausfather, Z., von der Heydt, A. S., Knutti, R., Mauritsen,  
1210 T., Norris, J. R., Proistosescu, C., Rugenstein, M., Schmidt, G. A., Tokarska, K. B., and  
1211 Zelinka, M. D.: An Assessment of Earth's Climate Sensitivity Using Multiple Lines of  
1212 Evidence, *Rev. Geophys.*, 58, e2019RG000678, <https://doi.org/10.1029/2019RG000678>,  
1213 2020.

1214 Skamarock, W. C., Klemp, J. B., Dudhia, J., Gill, D. O., Barker, D. M., Wang, W., and Powers, J. G.:  
1215 A description of the Advanced Research WRF Version 3. NCAR Tech Note NCAR/TN-  
1216 475+STR. NCAR, Boulder, CO, 2008.

1217 Tegen, I., Hollrig, P., Chin, M., Fung, I., Jacob, D., and Penner, J.: Contribution of different aerosol  
1218 species to the global aerosol extinction optical thickness: Estimates from model results,  
1219 *Journal of Geophysical Research: Atmospheres*, 102, 23895-23915,  
1220 <https://doi.org/10.1029/97JD01864>, 1997.

1221 Tewari, M., Wang, W., Dudhia, J., LeMone, M. A., Mitchell, K., Ek, M., Gayno, G., Wegiel, J., and  
1222 Cuenca, R.: Implementation and verification of the united NOAH land surface model in the  
1223 WRF model, 11-15 pp.2016.

1224 Thompson, G., Field, P. R., Rasmussen, R. M., and Hall, W. D.: Explicit Forecasts of Winter  
1225 Precipitation Using an Improved Bulk Microphysics Scheme. Part II: Implementation of a  
1226 New Snow Parameterization, *Monthly Weather Review*, 136, 5095-5115,  
1227 <https://doi.org/10.1175/2008MWR2387.1>, 2008.

1228 Tiedtke, M.: A Comprehensive Mass Flux Scheme for Cumulus Parameterization in Large-Scale  
1229 Models, *Monthly Weather Review*, 117, 1779-1800, 10.1175/1520-  
1230 0493(1989)117<1779:acmfsf>2.0.co;2, 1989.

1231 Torma, C., Giorgi, F., and Coppola, E.: Added value of regional climate modeling over areas  
1232 characterized by complex terrain—Precipitation over the Alps, *Journal of Geophysical*  
1233 *Research: Atmospheres*, 120, 3957-3972, 10.1002/2014JD022781, 2015.

1234 WCRP: CORDEX experiment design for dynamical downscaling of CMIP6 (DRAFT),  
1235 [https://cordex.org/wp-content/uploads/2020/06/CORDEX-  
CMIP6\\_exp\\_design\\_draft\\_20200610.pdf](https://cordex.org/wp-content/uploads/2020/06/CORDEX-<br/>1236 CMIP6_exp_design_draft_20200610.pdf), 2020.

1237 WCRP: CORDEX-CMIP6 Data Request, Coordinated Regional Downscaling Experiment  
1238 (CORDEX), [https://cordex.org/wp-content/uploads/2022/03/CORDEX-  
CMIP6\\_Data\\_Request\\_tutorial.pdf](https://cordex.org/wp-content/uploads/2022/03/CORDEX-<br/>1239 CMIP6_Data_Request_tutorial.pdf), 2022.

1240 Whetton, P. and Hennessy, K.: Potential benefits of a “storyline” approach to the provision of regional  
1241 climate projection information, International Climate Change Adaptation Conference,  
1242 NCARF, Gold Coast, Australia, 2010.

1243 Wilks, D. S.: “The Stippling Shows Statistically Significant Grid Points”: How Research Results are  
1244 Routinely Overstated and Overinterpreted, and What to Do about It, *Bulletin of the American*  
1245 *Meteorological Society*, 97, 2263-2273, <https://doi.org/10.1175/BAMS-D-15-00267.1>, 2016.

1246 Xie, K., Li, L., Chen, H., Mayer, S., Dobler, A., Xu, C. Y., and Gokturk, O. M.: Enhanced Evaluation  
1247 of Sub-daily and Daily Extreme Precipitation in Norway from Convection-Permitting Models  
1248 at Regional and Local Scales, *Hydrol. Earth Syst. Sci. Discuss.*, 2024, 1-38, 10.5194/hess-  
1249 2024-68, 2024.

1250 Zhuo, L., Dai, Q., Han, D., Chen, N., and Zhao, B.: Assessment of simulated soil moisture from WRF  
1251 Noah, Noah-MP, and CLM land surface schemes for landslide hazard application, *Hydrol.*  
1252 *Earth Syst. Sci.*, 23, 4199-4218, 10.5194/hess-23-4199-2019, 2019.

1253 Ziehn, T., Chamberlain, M. A., Law, R. M., Lenton, A., Bodman, R. W., Dix, M., Stevens, L., Wang,  
1254 Y.-P., and Srbinovsky, J.: The Australian Earth System Model: ACCESS-ESM1.5, *J. South*  
1255 *Hemisph. Earth Syst. Sci.*, 70, 193-214, <https://doi.org/10.1071/ES19035>, 2020.